THE JOURNAL OF BIOLOGICAL CHEMISTRY VOL. 291, NO. 51, pp. 26273–26290, December 16, 2016

Fibroblast Growth Requires CT10 Regulator of Kinase (Crk) and Crk-like (CrkL)*

Received for publication, October 25, 2016 Published, JBC Papers in Press, November 2, 2016, DOI 10.1074/jbc.M116.764613

Taeju Park[1], **Mateusz Koptyra, and Tom Curran**

From the Children's Research Institute, Children's Mercy Kansas City, Kansas City, Missouri 64108

Edited by Xiao-Fan Wang

CT10 regulator of kinase (Crk) and Crk-like (CrkL) are the cellular counterparts of the viral oncogene *v-Crk*. Elevated levels of Crk and CrkL have been observed in many human cancers; inhibition of Crk and CrkL expression reduced the tumor-forming potential of cancer cell lines. Despite a close relationship between the Crk family proteins and tumorigenesis, how Crk and CrkL contribute to cell growth is unclear. We ablated endogenous *Crk* and *CrkL* from cultured fibroblasts carrying floxed alleles of *Crk* and *CrkL* by transfection with synthetic Cre mRNA (*synCre*). Loss of Crk and CrkL induced by *synCre* transfection blocked cell proliferation and caused shrinkage of the cytoplasm and the nucleus, formation of adherens junctions, and reduced cell motility. Ablation of *Crk* or *CrkL* alone conferred a much more modest reduction in cell proliferation. Reintroduction of *CrkI*, *CrkII*, or *CrkL* individually rescued cell proliferation in the absence of the endogenous Crk and CrkL, suggesting that Crk and CrkL play overlapping functions in regulating fibroblast growth. Serum and basic FGF induced phosphorylation of Akt, MAP kinases, and S6 kinase and Fos expression in the absence of Crk and CrkL, suggesting that cells lacking Crk and CrkL are capable of initiating major signal transduction pathways in response to extracellular stimuli. Furthermore, cell cycle and cell death analyses demonstrated that fibroblasts lacking Crk and CrkL become arrested at the G_1-S transition and undergo a modest apoptosis. Taken together, our results suggest that Crk and CrkL play essential overlapping roles in fibroblast growth.

The chicken tumor virus oncoprotein, v-Crk, induces a substantial increase in protein tyrosine phosphorylation through protein-protein interactions mediated by its SH2[2] and SH3 domains, leading to cell transformation (1). CrkII and Crk-like (CrkL) represent closely related cellular homologues of v-Crk and have similar structures and functions (2). CrkI is a splice variant of CrkII that lacks the C-terminal SH3 domain. Crk family proteins (CrkI, CrkII, and CrkL) interact with many proteins through their SH2 and SH3 domains. Overexpression of Crk family proteins induces transformation of cultured cells (3, 4). *CrkI* is a more potent transforming gene than *CrkII* and *CrkL* in part because, like *v-Crk*, it lacks a C-terminal regulatory phosphorylation site (3). Overexpression of Crk and CrkL has been reported in several human cancers, including oral squamous cell carcinoma (5), ovarian carcinoma (6), colon cancer (7), lung cancer (8, 9), breast cancer (10, 11), gastric cancer (12), and glioblastoma (13, 14). Reduced expression of either Crk or CrkL by RNA interference-mediated knockdown lowered the *in vivo* tumor formation of human ovarian (15), synovial sarcoma (16), glioblastoma (14), breast cancer (10), head and neck squamous cell carcinoma (17), and rhabdomyosarcoma (18) cell lines. Taken together, these reports imply that elevated levels of Crk family proteins promote cell transformation and enhance tumor cell growth (for review see Refs. 19 and 20).

To investigate functions of endogenous Crk and CrkL in biological processes at the cellular level, we developed mouse strains and cell lines harboring individual and combined floxed alleles of *Crk* and *CrkL*. Application of the Cre-loxP recombination-based conditional knock-out approach to cultured fibroblasts enabled us to demonstrate that endogenous Crk and CrkL are important for maintaining cell structural integrity and proper cell motility (21). We also discovered that Crk and CrkL are required for cell transformation induced by viral oncogenes (22). Here we utilized the conditional knock-out system to examine whether endogenous Crk and CrkL are required for cell growth. Our findings clearly demonstrate that Crk and CrkL play essential, overlapping roles in fibroblast proliferation by enabling cells to progress from the G_1 phase to the S phase. Our study also demonstrates that expression of any one protein among CrkI, CrkII, and CrkL at physiological levels is sufficient to secure cell proliferation.

Results

Crk and CrkL Are Essential for Fibroblast Proliferation—We used the Neon system (Life Technologies) to achieve rapid and efficient gene expression in growing fibroblasts by transduction of synthetic mRNA (*synRNA*). To reduce innate immune responses and increase ectopic protein expression, we synthesized mRNA using the modified ribonucleotides, pseudo-UTP, and methyl-CTP (23, 24). When fibroblasts immortalized by T antigen or the 3T3 protocol were transfected with synthetic green fluorescent protein mRNA (*synGFP*), both cell types in monolayer cultures showed evidence of green fluorescence at 1 day post transduction (DPT) (Fig. 1*A*). As cells proliferated, the intensity of fluorescence in individual cells gradually decreased

* The authors declare that they have no conflicts of interest with the contents of this article.

[1] To whom correspondence should be addressed. Tel.: 816-302-8271; Fax: 816-983-6501; E-mail: tjpark@cmh.edu.

[2] The abbreviations used are: SH2 and SH3, Src homology domains 2 and 3; CrkL, Crk (CT10 regulator of kinase)-like; *synCre*, synthetic Cre mRNA; *synRNA*, synthetic mRNA; DPT, day(s) post transduction; *synGFP*, synthetic green fluorescent protein mRNA; HSP90, heat shock protein 90; ROI, region of interest.

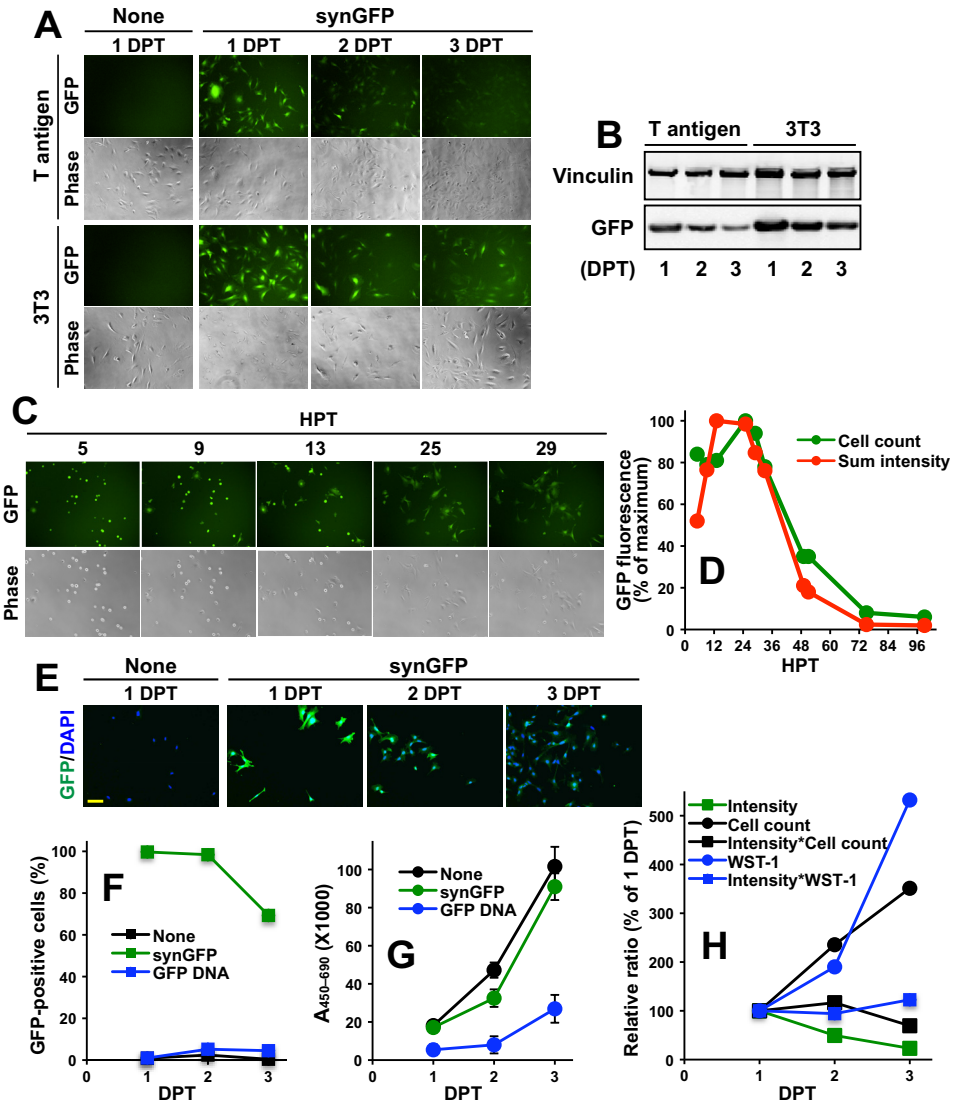

FIGURE 1. **Efficient and rapid expression of GFP after *synGFP* transfection.** *A–C*, *Crk/CrkL* double-floxed fibroblasts immortalized by T antigen or the 3T3 protocol were transfected without *synRNA* (*None*) or with *synGFP* (2 μg in 10 μl of cell suspension). *A*, both phase-contrast and GFP images of cells were taken at the indicated DPT. *B*, total cell lysates were obtained from cells transfected with *synGFP* for Western blot analyses. Protein levels of GFP at different DPT were compared. Vinculin levels were used as a control. *C* and *D*, T antigen-immortalized *Crk/CrkL* double-floxed fibroblasts were transfected with *synGFP* (2 μg in 10 μl cell suspension). At 5 h post transduction (*HPT*), GFP-positive cells were chosen, and time-lapse images of GFP and phase contrast were recorded every 4 h. The number of GFP-positive cells and their sum fluorescence intensities in the field of view were calculated using the Object Count function of the Nikon NIS element program. Four separate experiments were done, and a representative field of view was chosen for both image display (*C*) and GFP fluorescence quantification (*D*). *E–H*, T antigen-immortalized Crk/CrkL double-floxed fibroblasts were transfected without *synRNA* (*None*), with *synGFP* (2 μg in 10 μl cell suspension) or with GFP DNA (2 μg in 10 μl cell suspension). *E*, cells were fixed at the indicated DPT and stained with DAPI to visualize the nucleus. Representative images of GFP and DAPI are shown. *Scale bar*: 100 μm. *F*, the number of GFP-positive cells was counted (see "Experimental Procedures"). *G*, proliferation of fibroblasts after transfection was measured using WST-1. *H*, the average intensity of GFP fluorescence per cell for the *synGFP*-transfected cells (intensity) was calculated by combining all the sum fluorescence intensities in all the fields of view and dividing it by the total number of DAPI-positive objects. The total intensity was obtained by multiplying the average GFP fluorescence intensity per cell by the total number of DAPI-positive objects (intensity $\times$ cell count) or by the WST-1 measurement (intensity $\times$ WST-1).

(Fig. 1*A*). Similarly, the protein level of GFP in the cell population as measured by Western analysis displayed a similar trend (Fig. 1*B*). Time-lapse analysis of live fibroblasts transfected with *synGFP* showed strong GFP signals at 5 h post transduction, with the fluorescence reaching a maximum around 24 h post transduction, and thereafter, it gradually declined (Fig. 1, *C* and *D*). For quantification of the *synRNA* transfection efficiency, T antigen-immortalized fibroblasts were transfected with *synGFP* and fixed at different time points, and their nuclei were stained with DAPI. As shown in Fig. 1, *E* and *F*, 99 and 98% of fibroblasts were GFP-positive at 1 and 2 DPT, respectively. At 3 DPT, 69% of cells were positive for GFP. In contrast, only 5% of fibroblasts were GFP-positive at 2 and 3 DPT after GFP DNA transfection. The decrease in average GFP fluorescence intensity per cell over time is likely a consequence of the rapid proliferation of fibroblasts (Fig. 1*G*), thereby diluting the signal as the total intensities for all the fields of view (intensity $\times$ cell count) and the entire well (intensity x WST-1) stayed relatively constant over time (Fig. 1*H*). These observations suggest that electroporation of fibroblasts with *synRNA* is an effective method for rapid and efficient introduction of exogenous proteins into growing fibroblasts.

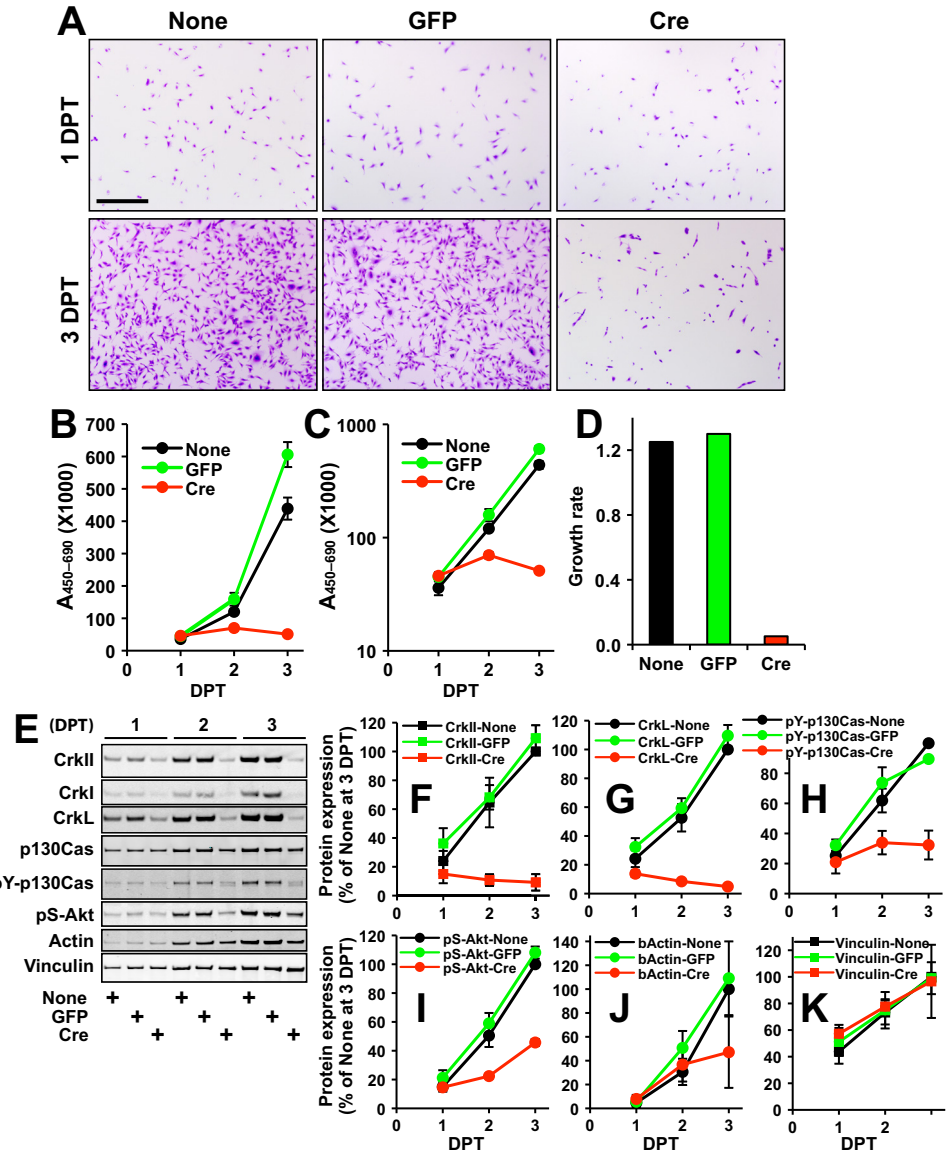

FIGURE 2. **Lack of cell proliferation in the absence of Crk and CrkL.** T antigen-immortalized *Crk/CrkL* double-floxed fibroblasts were transfected without *synRNA* (*None*) or with *synGFP* (*GFP*) or *synCre* (*Cre*) (2 μg in 10 μl of cell suspension). *A*, crystal violet images of cells were taken at the indicated DPT. Whereas control and *synGFP*-transfected fibroblasts had substantial proliferation, *synCre*-transfected cells failed to proliferate. *Scale bar*: 500 μm. *B* and *C*, cell proliferation was quantitatively measured using WST-1, and the $A_{450-690}$ values are presented in linear (*B*) and logarithmic (*C*) scales. *D*, exponential trend lines for the WST-1 assay graphs were drawn, and their slopes, the coefficients of *x*, are presented as the rates for exponential cell growth. *E*, total cell lysates were obtained at the indicated DPT for Western blot analyses. Protein levels were compared among cells transfected without *synRNA* (*None*) or with *synGFP* (*GFP*), or *synCre* (*Cre*). *F–K*, protein bands were quantified using the Odyssey system and calculated as percentages of the control (none at 3 DPT), and their mean ± S.D. values are shown in the graph.

To investigate the contribution of endogenous Crk and CrkL to cell growth, we immortalized fibroblasts from *Crk/CrkL* double-floxed mice using SV40 T antigen. We transfected the fibroblasts with synthetic Cre mRNA (*synCre*) to induce a rapid and efficient ablation of *Crk* and *CrkL*. As shown in Fig. 2*A*, staining of fibroblasts with crystal violet indicated substantial increases in cell number between 1 and 3 DPT for control and *synGFP*-transfected cells. In contrast, the cell number did not increase in cells transfected with *synCre*. Quantitative analyses of cell proliferation using WST-1 revealed similar exponential rates of cell proliferation in control and *synGFP* populations (slopes of 1.25 and 1.30, respectively) (Fig. 2, *B–D*). In contrast, *synCre* cells failed to proliferate (a slope of 0.05). Western analyses of cell lysates indicated that *synCre* induced efficient ablation of CrkI, CrkII, and CrkL. The steady state levels of Crk family proteins and other cellular proteins increased as control and *synGFP* cells recovered from trypsin-EDTA treatment and electroporation and continued to grow (Fig. 2*E*), probably due to increased cell-to-cell connections. It has been reported that expression and tyrosine phosphorylation of many cellular proteins, including focal adhesion proteins, increase at higher cell densities in Balb 3T3 fibroblasts (25). In contrast, in *synCre* cells, the levels of Crk family proteins declined after electroporation (Fig. 2, *E–G*). Tyrosine phosphorylation of p130Cas, a well known protein that associates

with Crk family members, decreased as Crk family proteins disappeared from the cells (Fig. 2, *E* and *H*). Phosphorylation of Akt was also reduced in the absence of Crk and CrkL (Fig. 2, *E* and *I*). Although the level of β-actin showed a modest decrease, vinculin expression was not affected by the loss of Crk and CrkL (Fig. 2, *J* and *K*). The requirement of Crk and CrkL for cell proliferation and p130Cas phosphorylation was also observed in fibroblasts immortalized by the 3T3 protocol, which grew more slowly than T antigen-immortalized fibroblasts (data not shown). Our results indicate that endogenous Crk and CrkL are required for proliferation of immortalized fibroblasts.

Morphological Alteration of Fibroblasts in the Absence of Crk and CrkL—Staining of fibroblasts with Crk and CrkL antibodies suggests that Crk is expressed in the nucleus and cytoplasm with a higher expression in the nucleus, whereas CrkL is expressed in both the cytoplasm and the nucleus at similar levels (Fig. 3*B*, data not shown). When cells were transfected with *synCre*, the level of Crk substantially declined. On the other hand, the decrease in the CrkL level was not obvious in part because a polyclonal antibody for CrkL was used for the staining, although Western blot analysis clearly showed a substantial change in CrkL levels between the control and *synCre* cells (Fig. 2, *E* and *G*, *versus* Fig. 3*B*). Staining polymerized actin with phalloidin indicated that actin stress fiber formation was defective in the absence of Crk and CrkL. Cytoplasmic staining with a heat shock protein 90 antibody showed well developed cellular processes in control fibroblasts that were lost in the absence of Crk and CrkL, resulting in a more rounded appearance (Fig. 3, *A* and *B*). Without Crk and CrkL, cells formed tight clusters (Fig. 3*A*) that could be dissociated by treatment with trypsin-EDTA (data not shown), suggesting that they are not multinucleated cells. Because overexpression of Crk caused breakdown of adherens junctions and cell spreading as well as decreased levels of two key components of the adherens junction, E-cadherin and p120-catenin, in Madin-Darby canine kidney epithelial and non-small cell lung cancer cells (26, 27), we tested whether adherens junction formation changed in fibroblasts lacking both Crk and CrkL. As shown in Fig. 3*B*, staining of control fibroblasts with a p120-catenin antibody did not exhibit any junctional structure between neighboring cells. In contrast, staining of *synCre*-transfected fibroblasts with the same antibody showed well developed adherens junctions between the neighboring cells (*yellow arrows* in Fig. 3*B*). However, the E-cadherin antibodies we tested did not show such a clear formation of adherens junctions. On the other hand, a pan-cadherin antibody displayed cell-to-cell junctions in both control and *synCre*-transfected cells, and the junctions looked more concentrated in *synCre* cells (*white arrows* in Fig. 3*B*). It is unclear whether they were adherens junctions because the shapes (*white arrows*) appeared to be different from the adherens junctions stained with p120-catenin (*yellow arrows*). Our results are consistent with Crk-induced breakdown of adherens junctions reported by Lamorte *et al.* (26) and suggest that adherens junctions were formed between neighboring cells in the absence of Crk and CrkL, contributing to formation of cell clusters. Furthermore, both nuclear and cytoplasmic areas of the cells significantly decreased in the absence of Crk and CrkL (Fig. 3, *C* and *D*). In addition, the cytoplasmic circularity increased in the absence of Crk and CrkL (Fig. 3*E*), suggesting that cells shrank and became rounded. Next, we examined whether the altered cell structure and formation of adherens junctions affect cell motility. The scratch wound-healing assay revealed directional migration of wild-type fibroblasts to the wound site for 24 h with 44 ± 4% of cells located in the region of interest (ROI) (Fig. 4, *A*–*C*). In contrast, only 4 ± 4% of *synCre*-transfected fibroblasts migrated to the wound site. These results confirm our previous findings (21) and demonstrate that Crk and CrkL play essential roles in cell structure, formation of cell-to-cell junctions, and cell motility.

Dose-dependent Effects of synCre—The highly efficient transduction of cells with *synCre* raised a potential concern of nonspecific toxicity of CRE. Previously, other groups associated high levels of CRE expression with inhibition of cell growth and cytopathic effects (28, 29). Therefore, we conducted a dose-response analysis of *synCre* in wild-type and *Crk/CrkL* double-floxed fibroblasts. Transfection of wild-type fibroblasts with *synCre* up to 0.2 μg did not affect exponential growth of cells (Fig. 5, *A* and *C*). However, use of 0.66 μg and more of *synCre* reduced proliferation of wild-type cells in a dose-dependent manner. In contrast, as little as 0.066 μg of *synCre* inhibited proliferation of Crk/CrkL double-floxed cells, and at 0.2 μg there was essentially no growth (Fig. 5, *B* and *C*). Crystal violet staining of *Crk/CrkL* double-floxed cells showed that both inhibition of cell proliferation and morphological alteration occurred at a level of 0.2 μg *synCre,* indicating that both phenotypes are related (Fig. 5*D*). Examination of CrkI, CrkII, and CrkL indicated that all were effectively ablated using as little as 0.2 μg of *synCre* in double-floxed cells (Fig. 5, *E*–*G*). Furthermore, the changes in the growth rate and in the Crk family protein levels were closely correlated in *Crk/CrkL* double-floxed cells (Fig. 5, *C versus F* and *G*), suggesting that Crk family proteins play an essential role in cell proliferation. Phosphorylated forms of p130Cas and Akt were decreased to similar extents by 0.2 μg of *synCre* (Fig. 3, *H* and *I*). On the other hand, the decrease in β-actin levels induced by 2 μg *synCre* in wild-type cells seems to reflect a nonspecific effect of *synCre*. These results suggest that 0.2 μg is the optimal amount of *synCre* to investigate the effects of Crk/CrkL ablation without confounding nonspecific effects of high levels of CRE. Therefore, we chose to use 0.2 μg of *synCre* for further analyses.

Independent Roles of Crk or CrkL in Cell Growth—Because transfection of *Crk/CrkL* double-floxed cells with *synCre* ablated both *Crk* and *CrkL*, it was unclear which of these proteins was actually required for cell proliferation. To ablate *Crk* or *CrkL* alone, we derived immortalized fibroblasts from *Crk* or *CrkL* floxed mice and transfected them with *synCre*. As shown in Fig. 6, *A* and *B*, loss of either Crk or CrkL only slightly reduced cell proliferation (10.8% and 4.9% inhibition for single-floxed cells compared with 92.4% for double-floxed cells). Furthermore, loss of either Crk or CrkL did not result in any detectable morphological alterations (Fig. 6*C*). Western analyses verified the loss of Crk or CrkL alone upon *synCre* transfection in single-floxed cells (Fig. 6, *D* and *E*). It is noteworthy that phosphorylated p130Cas decreased only when cells lost Crk (or

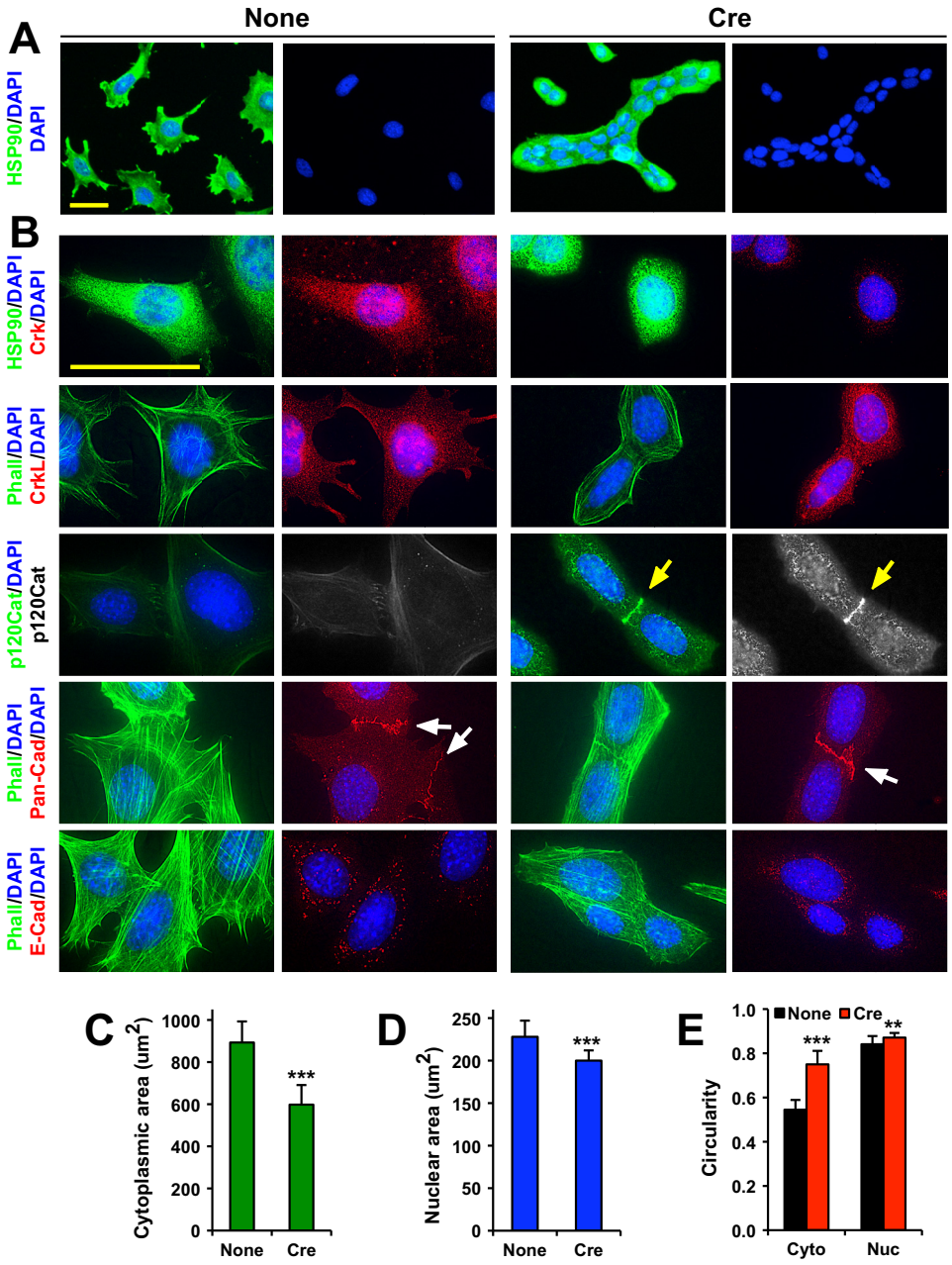

FIGURE 3. **Morphological alterations of cells in the absence of Crk and CrkL.** T antigen-immortalized Crk/CrkL double-floxed fibroblasts were transfected without *synRNA* (*None*) or with *synCre* (0.2 μg in 10 μl cell suspension). At 3 DPT, cells were fixed and stained with antibodies and DAPI to visualize distribution of proteins and identify the cytoplasm and the nucleus. *A*, cells were immunostained with a *HSP90* antibody to visualize the cytoplasm. *Scale bar*: 50 μm. *B*, cells were immunostained with Crk, CrkL, p120-catenin, pan-cadherin, and E-cadherin antibodies to visualize distribution of the proteins. Cells were also co-stained with a HSP90 antibody and phalloidin to visualize the cytoplasm and actin stress fibers, respectively. *Yellow* and *white arrows* indicate formation of cell-to-cell junctions. *C*, areas of DAPI-stained objects were calculated (see "Experimental Procedures"), and their mean ± S.D. values are shown. *D*, areas of HSP90-stained objects were calculated (see "Experimental Procedures"), and their mean ± S.D. values are shown. *E*, the circularity (roundness) of the cytoplasm (*Cyto*) and nucleus (*Nuc*) was measured (see "Experimental Procedures"), and their mean ± S.D. values are shown. ***, $p < 0.001$; **, $p < 0.01$, compared with control.

Crk plus CrkL). The result suggests that Crk predominantly mediates phosphorylation of p130Cas. Phosphorylation of Akt decreased in the absence of both Crk and CrkL, but it did not decrease significantly when cells lacked either Crk or CrkL, suggesting that both Crk and CrkL contribute to Akt phosphorylation, with either sufficient for the phosphorylation to occur. The results from single-floxed fibroblasts demonstrate that Crk and CrkL play overlapping functions in cell proliferation and that ablation of one does not cause obvious defects.

Rescue of Cell Proliferation by Reintroduction of Crk Family Proteins—To assess the contribution of individual Crk family proteins as well as SH2 and SH3 domains to cell proliferation, we co-transfected Crk/CrkL double-floxed cells with *synCre* plus various Crk and CrkL constructs (Fig. 7*A*) to introduce exogenous genes in the absence of the endogenous Crk and CrkL. Transfection of Crk/CrkL double-floxed cells with various Crk/CrkL constructs without *synCre* did not affect cell morphology or proliferation (*top panels* of Fig. 7, *B* and *C* and

Fig. 7, *D* and *F*). Both the morphological alterations and failure of cell proliferation that were caused by loss of Crk and CrkL upon *synCre* introduction were effectively reversed when cells were co-transfected with wild-type *CrkI*, *CrkII*, or *CrkL* (*bottom panels* of Fig. 7, *B* and *C*, and Fig. 7, *E* and *F*). Western analyses confirmed the loss of endogenous CrkI, CrkII, and CrkL in the presence of *synCre* plus any one of the Crk family proteins (Fig. 7, *G* and *H*). Exogenous CrkII and CrkI, whose protein levels were 145 and 61%, respectively, of the endogenous CrkII level, were able to fully rescue cell proliferation. The full rescue by both CrkII and CrkI suggests that the C-terminal SH3 domain that is absent in CrkI does not play a significant role in cell proliferation. Exogenous CrkL, whose protein level was 108% of the endogenous CrkL, also rescued cell proliferation. Taken together, the results indicate that cells can proliferate normally if any of the Crk proteins is present at a level approximately half that of endogenous CrkII or CrkL.

Both CrkII and CrkL, but not CrkI, have conserved tyrosine residues (Tyr-221 and Tyr-207, respectively) in the linker region between the two SH3 domains. Phosphorylation of these tyrosine residues by kinases such as Abl and Arg followed by an intramolecular interaction with the SH2 domain and reduced accessibility of both the SH2 and N-terminal SH3 domains to their binding partners is known to contribute to decreased transforming activities of CrkII and CrkL (30, 31). Therefore, we tested whether phosphorylation of the regulatory tyrosine residues affects cell proliferation. Phosphotyrosine mutants between the N- and C-terminal SH3 domains of CrkII and CrkL, CrkIIY221F and CrkLY207F, rescued cell proliferation substantially but to a lesser extent than the wild-type proteins (Fig. 7, *E* and *F*). The substantial rescue by CrkIIY221F suggests that phosphorylation of Tyr-221 may not be required for cell proliferation. Considering that the level of CrkIIY221F was 131% that of the endogenous CrkII, the phosphotyrosine mutant seems to be less effective than the wild-type despite lack of an intramolecular interaction between the tyrosine residue and the SH2 domain. The substantial rescue by CrkLY207F, although its expression level was 32% that of the endogenous CrkL, suggests that phosphorylation of CrkL at Tyr-207 is not essential for cell proliferation. Next we tested whether cells require both SH2 and SH3 domains to proliferate. The presence of both the SH2 and N-terminal SH3 domains of Crk is essential for growth as both CrkIIR38K and CrkIIW169K failed to rescue cell proliferation (Fig. 7, *E* and *F*). The modestly higher growth rate of cells expressing CrkIIW275K, a mutant in the C-terminal SH3 domain, may reflect higher residual levels of endogenous Crk family proteins and/or a lower expression level of the mutant. Taken together, our results suggest that CrkI, CrkII, and CrkL play essential overlapping roles in cell proliferation through their SH2 and N-terminal SH3 domains.

Failure of Cell Proliferation Despite c-Jun N-terminal Kinase (JNK) Reintroduction—JNK family members have often been implicated in Crk signaling (32). For example, JNKs and Crk proteins participate in endothelin-1 signaling in cardiomyocytes (33), vascular endothelial growth factor receptor-3-induced signaling in primary human umbilical vein endothelial cells (34), and the *Drosophila* homolog of the PDGF/VEGF receptor (PVR)-induced thorax closure during *Drosophila* metamorphosis (35). Cell transformation induced by v-Crk requires JNK activity (36, 37) and Met-induced fibroblast transformation is correlated with Crk-mediated JNK activation (38, 39). Therefore, we examined whether JNK phosphorylation was altered in the absence of Crk and CrkL. In wild-type fibroblasts, JNK phosphorylation was not altered in the presence of up to 0.66 μg *synCre* (Fig. 8, *A* and *B*). In contrast, JNK phosphorylation decreased dramatically in a dose-dependent manner in the presence of *synCre*, similar to the drop in CrkII and CrkL in double-floxed fibroblasts (Fig. 8, *A* and *B*, *versus* Fig. 5, *C*, *F*, and *G*). Vinculin levels, however, were not affected by *synCre* (Fig. 8*A*). Next we tested to see whether the expression of constitutively active JNKs could rescue cell proliferation in the absence of Crk and CrkL. Although transfection of fibroblasts with synthetic mRNA for MKK-JNK1 and MKK-JNK2 (40) induced low levels of protein expression and phosphorylation, transfection of the corresponding DNAs led to higher levels of expression (Fig. 8*F*). Co-transfection of *Crk/CrkL* double-floxed fibroblasts with constitutively active *JNK1* and *JNK2*

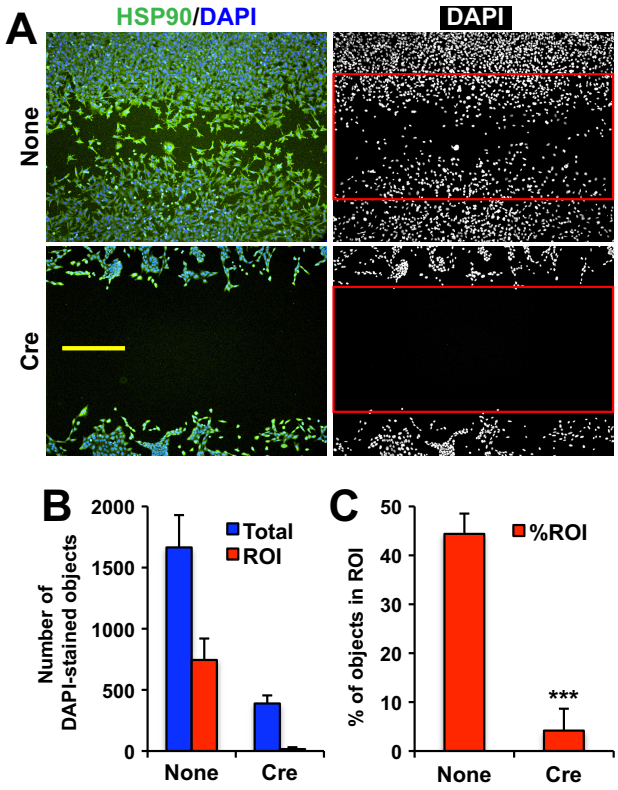

FIGURE 4. **Reduced cell motility in the absence of Crk and CrkL.** T antigen-immortalized *Crk/CrkL* double-floxed fibroblasts were transfected without *synRNA* (*None*) or with *synCre* (0.2 μg in 10 μl cell suspension). At 2 DPT, a wound was created by scratching through the cell monolayer with a micropipette tip, and cells were allowed to migrate into the gap at the wound site for 24 h, fixed, and stained with a HSP90 antibody and DAPI to visualize the cytoplasm and nucleus. *A*, after fluorescence images were taken, a ROI of 2230 $\times$ 1000 μm as the original wound gap was drawn (*red rectangles*) using the Nikon NIS element program. Six separate experiments were done for each group, and representative images are shown. *Scale bar*: 500 μm. *B*, DAPI-stained objects were counted using the Nikon NIS element program for the whole image and for the ROI. Data are shown as the mean $\pm$ S.D. (*bars*) values. *C*, the percentage of cells that migrated to the ROI was calculated for each image. Data are shown as the mean $\pm$ S.D. (*bars*) values. ***, $p < 0.001$, compared with control.

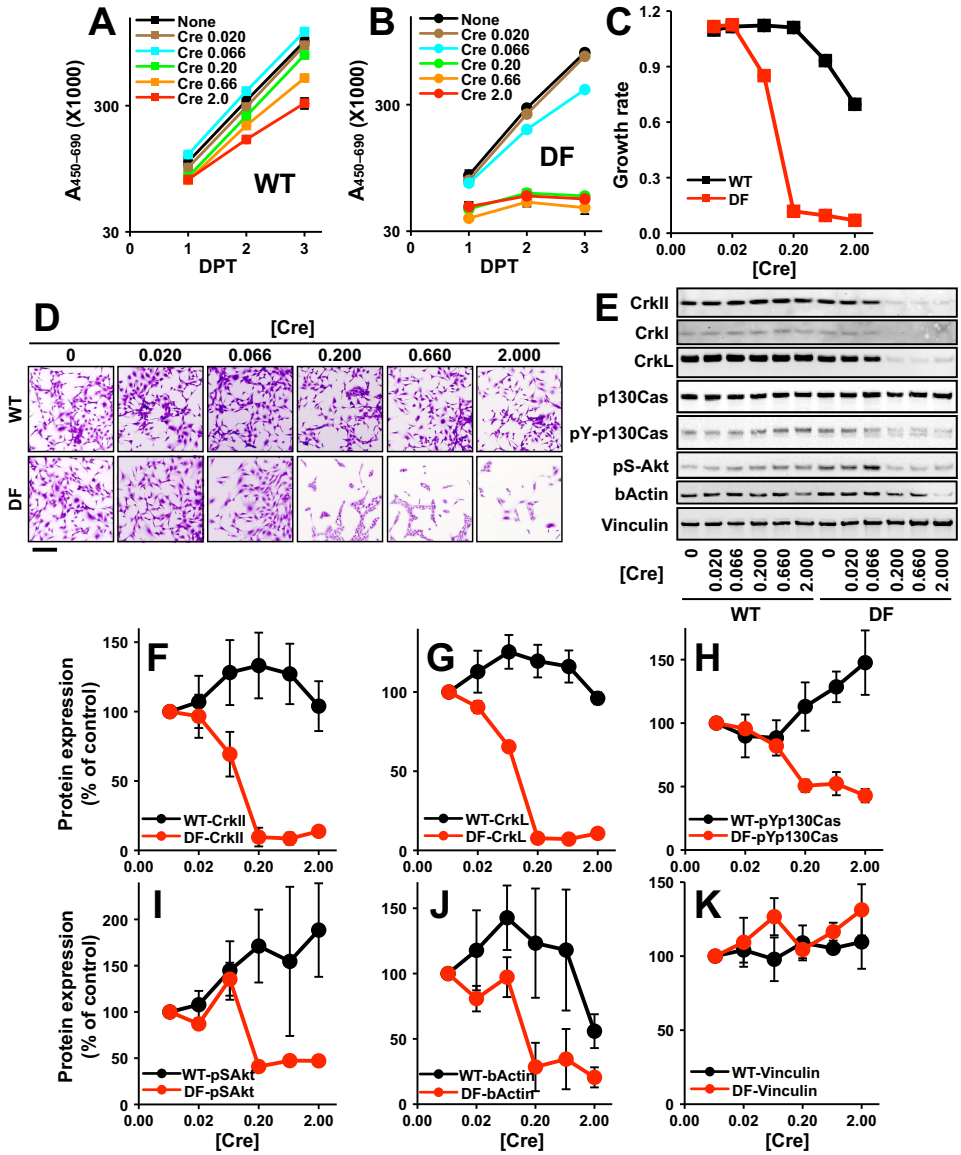

FIGURE 5. **synCre concentration-dependent inhibition of cell proliferation.** Wild-type (*WT*, *A*) and *Crk/CrkL* double-floxed (*DF*, *B*) fibroblasts immortalized by T antigen were transfected with increasing concentrations of *synCre* (μg in 10 μl cell suspension), and their cell proliferation was measured using WST-1. *C*, an exponential trend line for the WST-1 assay graph was drawn, and its slope, the coefficient of *x*, is presented as the rate for exponential cell growth. *D*, cells that were transfected with indicated concentrations of *synCre* were fixed at 3 DPT, and crystal violet images of cells were taken. *Scale bar*: 200 μm. *E*, total cell lysates were obtained from cells transfected with indicated concentrations of *synCre* at 3 DPT for Western blot analyses. Protein levels were compared among different *synCre* concentrations. *F–K*, protein bands were quantified using the Odyssey system, and their mean ± S.D. values are shown.

synRNA or DNA together with *synCre* led to various levels of expression and phosphorylation of JNK1 and JNK2 (Fig. 8*F*). Co-transfecting cells with *CrkII*, but not constitutively active JNK1, rescued proliferation of *synCre*-transfected cells (Fig. 8, *C* and *D*). Surprisingly, we found that expression of activated JNK2 interfered with CRE recombinase activity, resulting in incomplete elimination of Crk proteins in transfected cells. To avoid interference between JNKs and CRE, we first transfected Crk/CrkL double-floxed fibroblasts with *synCre* then 12 h later we transfected the cells with constitutively active JNKs. Western analyses showed that endogenous Crk family proteins were effectively removed by the initial *synCre* transfection. The subsequent transfection of cells with constitutively active JNKs enabled expression and phosphorylation of both JNK1 and JNK2 (Fig. 8*G*); however, expression of constitutively active JNKs was not sufficient to rescue cell proliferation in the absence of Crk and CrkL (Fig. 8*H*). Furthermore, a second transfection with wild-type, dominant negative, and constitutively active forms of JNK1, JNK2, or both did not rescue cell proliferation in the absence of Crk and CrkL (data not shown). These results suggest that although JNK phosphorylation dramatically declines in the absence of Crk and CrkL, activation of JNKs alone is not sufficient to drive cell proliferation in the absence of Crk and CrkL.

Capability of Activating Signal Transduction Pathways in the Absence of Crk and CrkL—To gain insights into the mechanism underlying the blockage of cell proliferation in the absence of Crk and CrkL, we examined whether cells lacking Crk and CrkL were capable of responding to extracellular stimuli. Several growth factors have been reported to stimulate proliferation of fibroblasts (41–43). In addition, Crk and CrkL are known to be

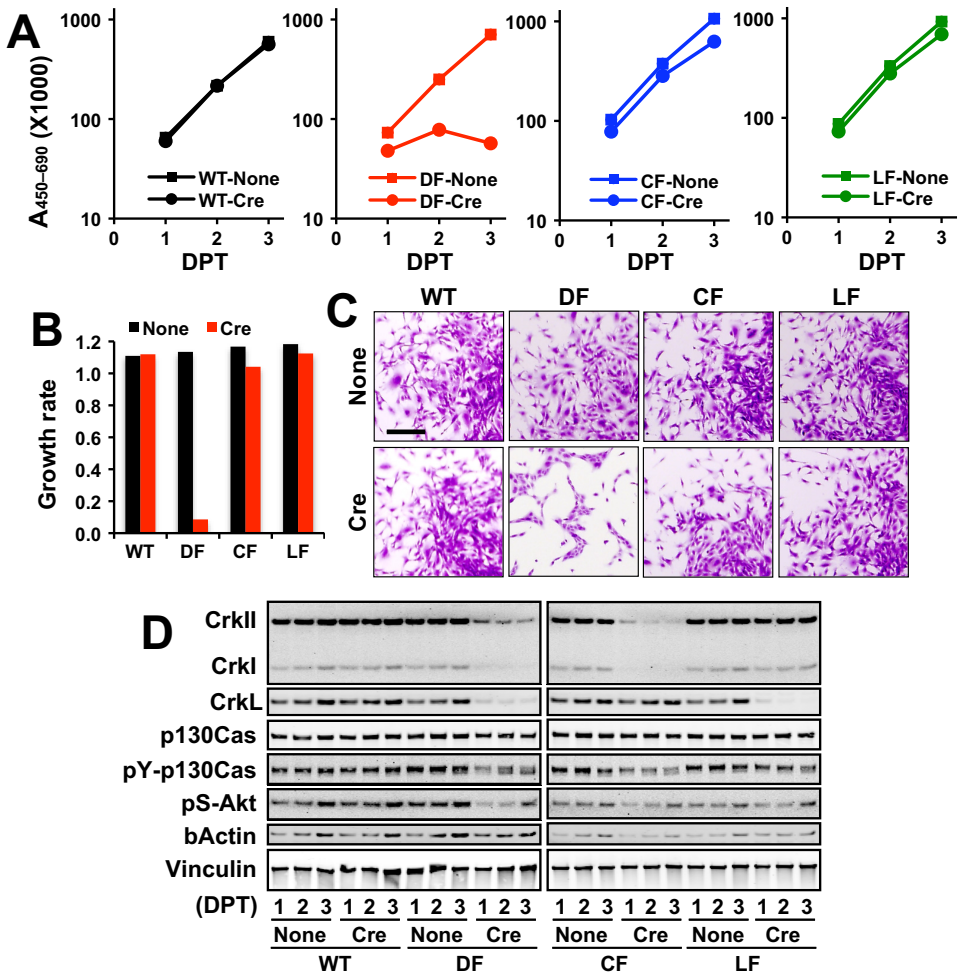

FIGURE 6. **Cell proliferation in the absence of either Crk or CrkL.** *A*, wild-type (*WT*), *Crk/CrkL* double-floxed (*DF*), *Crk* floxed (*CF*), and *CrkL* floxed (*LF*) fibroblasts immortalized by T antigen were transfected with *synCre* (0.2 μg in 10 μl of cell suspension), and their cell proliferation was measured using WST-1. *B*, an exponential trend line for the WST-1 assay graph was drawn, and its slope, the coefficient of *x*, is presented as the rate for exponential cell growth. *C*, crystal violet images of cells transfected without *synRNA* (*None*) or with *synCre* (*Cre*) were taken at 3 DPT. *Scale bar*: 200 μm. *D*, total cell lysates were obtained from cells at 3 DPT for Western blot analyses. Protein levels were compared between control and *synCre*-transfected cells. *E*, protein bands were quantified using the Odyssey system, calculated as percentages of the control (None at 1 DPT), and their mean ± S.D. values are shown.

required for PDGF-stimulated remodeling of the actin cytoskeleton and cell migration (44). At first we cultured fibroblasts in low serum (0.5% FBS) for 4 days. Whereas control fibroblasts grew for 3 days and stopped growing probably due to depletion of nutrients, *synCre*-transfected cells failed to grow in low serum (Fig. 9*A*). The addition of EGF, PDGF, and basic FGF stimulated proliferation of control fibroblasts, which became apparent 4 days after growth factor treatment (Fig. 9, *B–D*). We also tested IGF-I, but it did not stimulate cell proliferation under our experimental conditions (data not shown). Although both PDGF and basic FGF were able to stimulate proliferation of *synCre*-transfected cells, the effect of EGF on cell proliferation diminished 4 days after treatment. The results suggest that serum and EGF, but not PDGF or basic FGF, require Crk and CrkL to induce cell proliferation. Because cells were capable of proliferating in response to some growth factors, we examined whether major signal transduction pathways function in the absence of Crk and CrkL. When control fibroblasts were stimulated with high serum (20% FBS) after a day with low serum (0.5% FBS), there was a rapid onset of phosphorylation of Akt, MAP kinases (ERK, JNK, and p38), and S6 kinase in 5 min as well as induction of Fos expression in an hour (Fig. 9*E*). Cells transfected with *synCre* exhibited similar biochemical changes. Basic FGF, which evoked the highest response in cell proliferation among the tested growth factors, induced phosphorylation of MAP kinases and Fos induction in both control and *synCre*-transfected cells. These results suggest that cells lacking Crk and CrkL are capable of initiating major signal transduction pathways.

Cell Cycle Arrest and Apoptosis—We explored whether the failure in cell proliferation observed in the absence of Crk and CrkL was caused by changes in cell cycle. Cells were fixed with ethanol, stained with propidium iodide, and subjected to flow cytometry analysis. Cells transfected with *synCre* showed significant increases in the G_1 phase and significant decreases in the S and G_2/M phases compared with control cells at 2 and 3 DPT (Fig. 10, *A* and *B*). At 3 DPT, cells at G_1 increased from 35.3 ± 1.6% to 45.0 ± 3.7%, whereas cells at S decreased from 22.1 ± 0.6% to 9.8 ± 0.1%. Cells at G_2/M also decreased from 34.0 ± 1.8% to 21.8 ± 1.2% at 3 DPT. These results suggest that cells lacking Crk and CrkL become arrested at the G_1-S transition. In addition, a modest but significant increase of sub-G_1 cells after *synCre* transfection (from 1.8 ± 0.4% to 6.9 ±

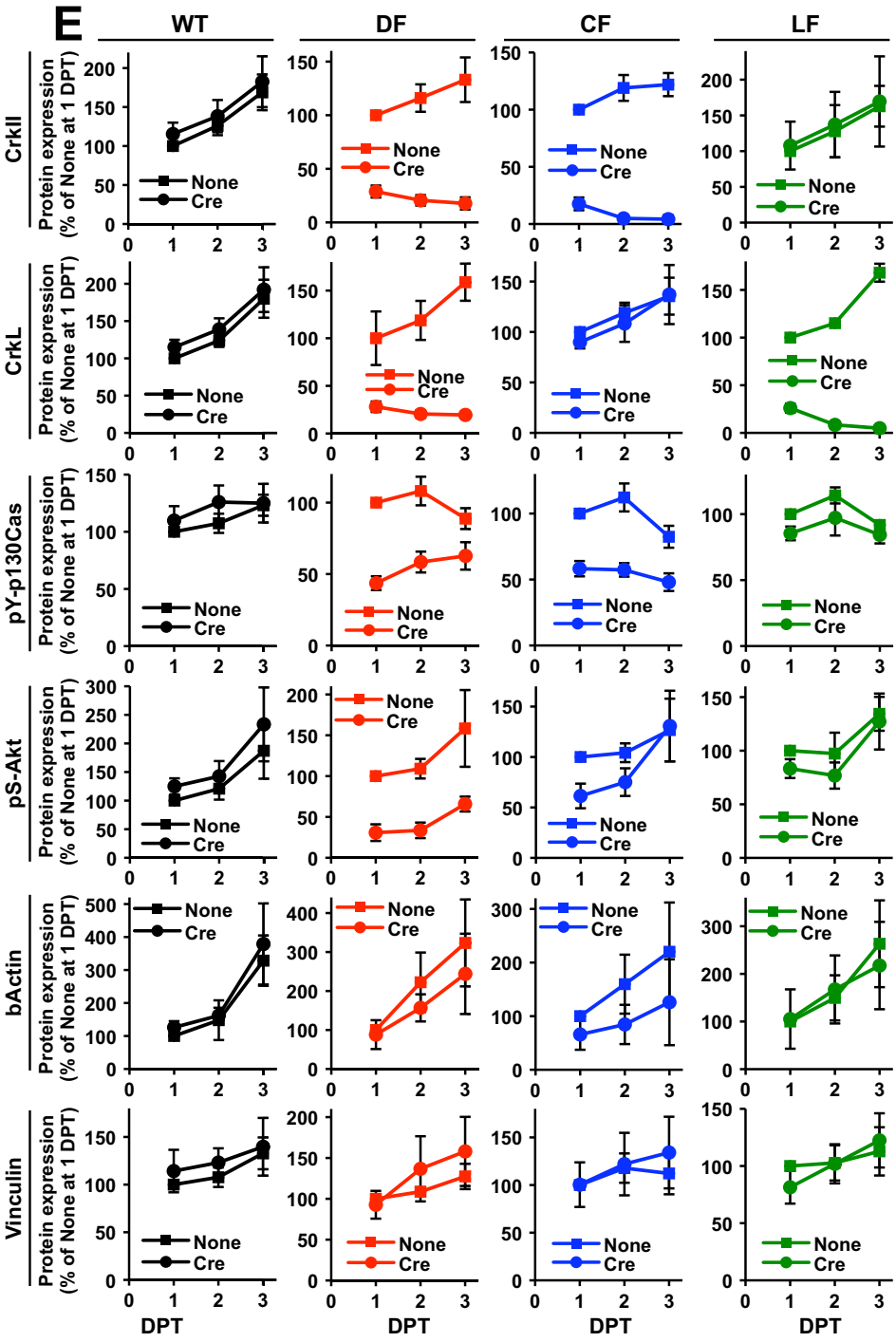

FIGURE 6—*continued*

1.5% at 3 DPT) may indicate the cell death as a consequence of Crk and CrkL removal. Western blot analyses did not detect any of the two apoptosis markers, cleaved caspase 3 and cleaved PARV, in synCre-transfected cells at 3 DPT (data not shown). Then we stained live cells with annexin V and propidium iodide to examine whether cells undergo apoptosis and necrosis in the absence of Crk and CrkL. As shown in Fig. 11, *A* and *C*, annexin V-positive cells significantly increased after *synCre* transfection at 3 DPT (from 4.7 ± 0.4% to 9.8 ± 1.3%). On the other hand, propidium iodide-positive cells slightly, but not significantly, increased after *synCre* transfection at 3 DPT (from 4.3 ± 0.4% to 6.2 ± 1.1%) (Fig. 11, *B* and *D*). These results suggest that fibroblasts lacking Crk and CrkL undergo a modest apoptosis.

Discussion

Because their identification as cellular counterparts of the viral oncogene *v-Crk*, Crk and CrkL have been extensively studied for their roles in cell growth and tumorigenesis. Overexpression of Crk and CrkL in human cancers and their requirement for *in vivo* tumor formation by several cancer cell lines

suggest that they contribute to cell transformation as well as aberrant growth and motility of tumor cells. However, it was unclear whether Crk and CrkL proteins, expressed at normal endogenous levels, contribute to cell growth and tumorigenesis. Previously, we reported that endogenous Crk and CrkL proteins are important for cell motility and structural integrity and that cells undergo severe structural alterations in the absence of Crk and CrkL (21). Furthermore, we demonstrated that endogenous Crk and CrkL are required for cell transformation induced by viral oncogenes such as *v-fos* and *v-ras* (22). Here, we demonstrate that endogenous Crk and CrkL proteins play essential roles in fibroblast growth. Loss of both Crk and CrkL

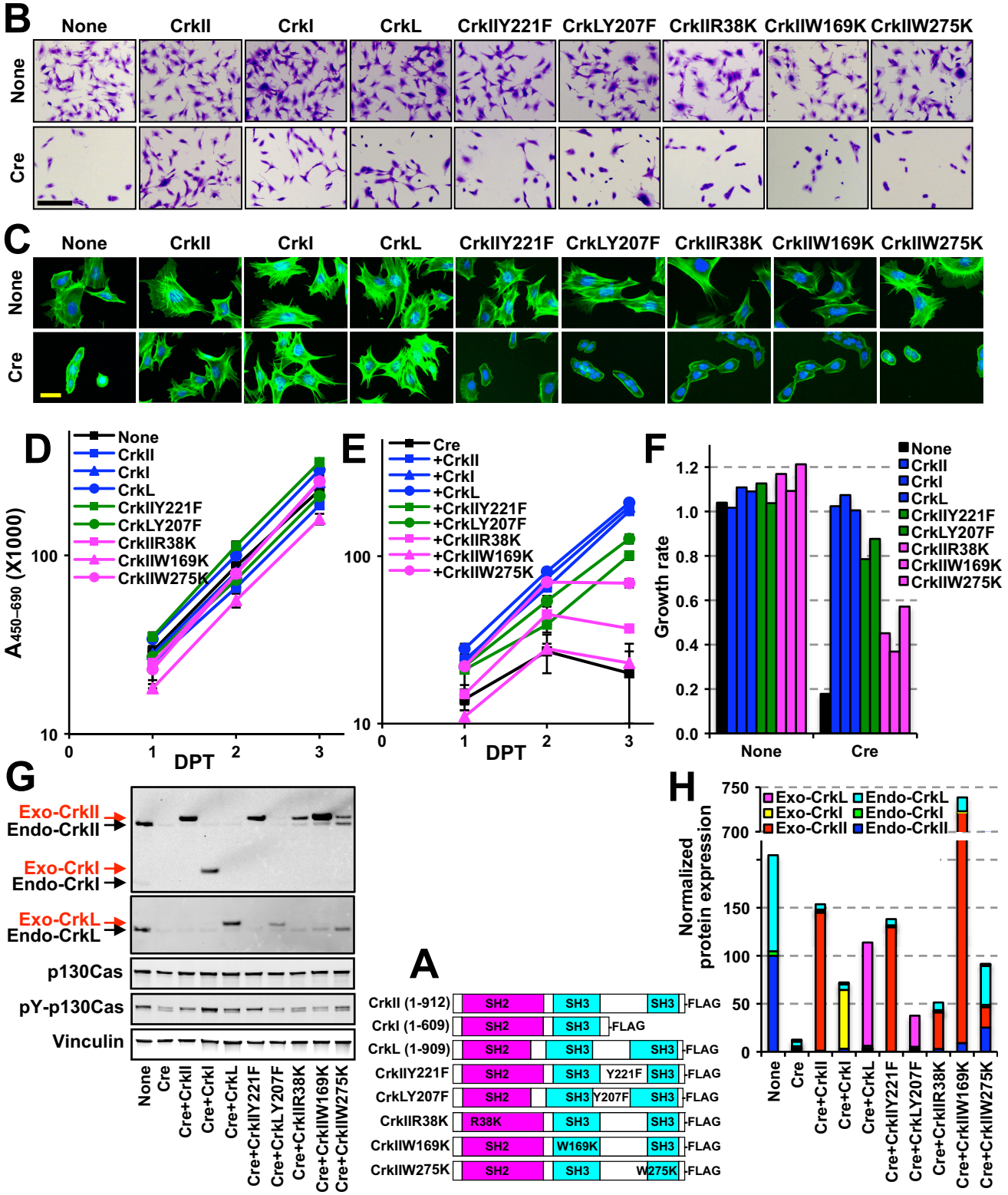

caused a complete failure of cell proliferation, although the absence of either Crk or CrkL only slightly affected that process. Reintroduction of exogenous CrkII, CrkI, or CrkL individually, in the absence of endogenous Crk and CrkL, rescued cell proliferation, supporting the hypothesis that expression of any member of the Crk family proteins is sufficient for cell proliferation. Cell cycle analyses of fibroblasts lacking Crk and CrkL indicate that cells become arrested at G_1. The link between the cell cytoskeleton and cell cycle is not a new idea. Huang and Ingber (45) reported that prevention of human capillary endothelial cells from spreading and subsequent cell shape changes blocked cell cycle progression from G_1 to S, with a failure of the following biochemical changes: an increase in cyclin D1 protein levels, down-regulation of the cell cycle inhibitor p27Kip1, and phosphorylation of the retinoblastoma protein. In addition, pharmacological disruption of the actin cytoskeleton blocked the G_1-S transition in human capillary endothelial cells and mammalian fibroblasts (46, 47). It is unclear whether the decrease in actin protein levels we observed in the absence of Crk and CrkL contributes to the cell cycle arrest, partly because the change in actin levels was not always consistent and correlated with loss of Crk and CrkL unlike protein levels and phosphorylation of p130Cas. Those reports about the importance of the cell cytoskeleton in the cell cycle together with our previous report on the essential roles of Crk and CrkL in maintaining the cell cytoskeleton (21) suggest that Crk and CrkL play a critical role in cell cycle progression by controlling the cell cytoskeleton. Further studies would be needed to define the detailed mechanism. All in all, our previous and present results demonstrate that Crk and CrkL play essential roles in structural integrity, cell motility, cell transformation, and cell cycle in cultured fibroblasts. Our findings might help to develop a novel approach for therapeutic intervention in cancer. A clear understanding of the detailed mechanism responsible for cell proliferation mediated by endogenous or elevated levels of Crk and CrkL together with development of an effective and therapeutically feasible deletion of Crk and CrkL from cells will be essential for this goal. In addition, we need to investigate whether normal and transformed cells are different in the dependence on Crk and CrkL for proliferation.

Cell growth seems to require a threshold level of Crk family proteins; cells proliferate above the threshold, and increased expression does not stimulate cell proliferation further. Each Crk family protein alone is sufficient to drive cell proliferation. Previously, we were able to show that a human podocyte cell line does not distinguish between CrkII and CrkL for nephrine-induced lamellipodia formation, as we observed recovery of lamellipodia formation upon CrkII overexpression in CrkL knockdown cells and upon CrkL overexpression in CrkII knockdown cells (48). In that case, the threshold for Crk family proteins was higher, and removal of one protein caused defects, which could be rescued by overexpressing the other member. This study reaffirms that our approach is very effective in defining distinct and overlapping functions of Crk and CrkL. Many overlapping functions of Crk and CrkL have been uncovered by a close examination of individual and combined knock-out of Crk and CrkL (48–51).

The biochemical changes in the absence of Crk, CrkL, or both (Fig. 6) shed light on analyzing which signaling molecules or signal transduction pathways are involved in Crk/CrkL-mediated cell proliferation. Phosphorylation of p130Cas was rapidly decreased in the absence of both Crk and CrkL, a finding that correlated well with the levels of Crk and CrkL as well as the degree of cell proliferation. However, the observation that p130Cas phosphorylation, but not cell proliferation, was affected by the absence of Crk alone makes it difficult to conclude that p130Cas phosphorylation is a good indicator of Crk/CrkL-dependent cell proliferation. On the other hand, phosphorylation of Akt decreased in the absence of both Crk and CrkL, and the decrease was not significant when cells lacked either Crk or CrkL. However, Akt phosphorylation was not blocked completely in the absence of both Crk and CrkL, and it modestly increased at 3 DPT. Therefore, it is unclear whether Akt activity is directly connected to Crk family protein levels. MAP kinases have been implicated in Crk/CrkL-mediated signaling pathways (33–36, 38, 52). The levels of phosphorylated JNKs were reduced when cells lost Crk and CrkL (Fig. 8). Cotransfection of cells with *synCre* plus constitutively active JNKs suggested that JNK activation cannot rescue cell proliferation. These steady state levels of protein phosphorylation are different from the results from a short term stimulation of cells with serum and basic FGF. Increased phosphorylation of Akt, MAP kinases (ERK, JNK and p38), and S6 kinase and Fos expression were induced in response to serum and basic FGF regardless of Crk and CrkL ablation (Fig. 9, *E–H*). It is less clear what causes the difference in steady state levels and short term responses of signaling molecules. On the other hand, cell cycle arrest of fibroblasts lacking Crk and CrkL at G_1 points a new direction for the study of Crk/CrkL, although it is unclear how Crk and CrkL control the cell cycle. The existence of numerous Crk/CrkL-interacting proteins poses a great challenge in identifying specific proteins and pathways downstream of Crk/CrkL that drive cell proliferation. Potentially, Crk and CrkL may orchestrate multiple pathways for coordinated regulation of cell structure, motility, and cell cycle. Therefore, a systematic approach to identifying downstream

FIGURE 7. **Recovery of cell proliferation by reintroduction of Crk and CrkL.** T antigen-immortalized *Crk/CrkL* double-floxed (*DF*) fibroblasts were co-transfected with *synCre* (0.2 μg in 10 μl cell suspension) plus various Crk and CrkL constructs (2 μg of *synRNA* in 10 μl cell suspension), and their cell proliferation was measured using WST-1. *A*, schematic diagrams of various Crk and CrkL constructs. *B*, crystal violet images of cells transfected with various Crk and CrkL constructs with or without *synCre* were taken at 3 DPT. *Scale bar*: 200 μm. *C*, cells were fixed at 3 DPT and stained with phalloidin and DAPI to visualize actin stress fibers and the nucleus, respectively. *D*, proliferation of cells transfected with various Crk and CrkL constructs without *synCre* was measured using WST-1. *E*, proliferation of cells transfected with various Crk and CrkL constructs plus *synCre* was measured using WST-1. *F*, an exponential trend line for the WST-1 assay graph was drawn, and its slope, the coefficient of *x*, is presented as the rate for exponential cell growth. *G*, total cell lysates were obtained from cells at 3 DPT for Western blot analyses. Protein levels were compared among control, *synCre*-transfected cells and cells transfected with *synCre* plus various Crk and CrkL constructs. *H*, protein bands were quantified using the Odyssey system, and their mean ± S.D. values are shown in the graph. The protein levels of endogenous CrkII and CrkL in control cells served as references and were assigned 100% each, and relative protein levels of endogenous and exogenous proteins in cells expressing CRE and various Crk and CrkL constructs are normalized to their references. The steady state protein level of endogenous CrkI was ~5% that of endogenous CrkII in normal cells.

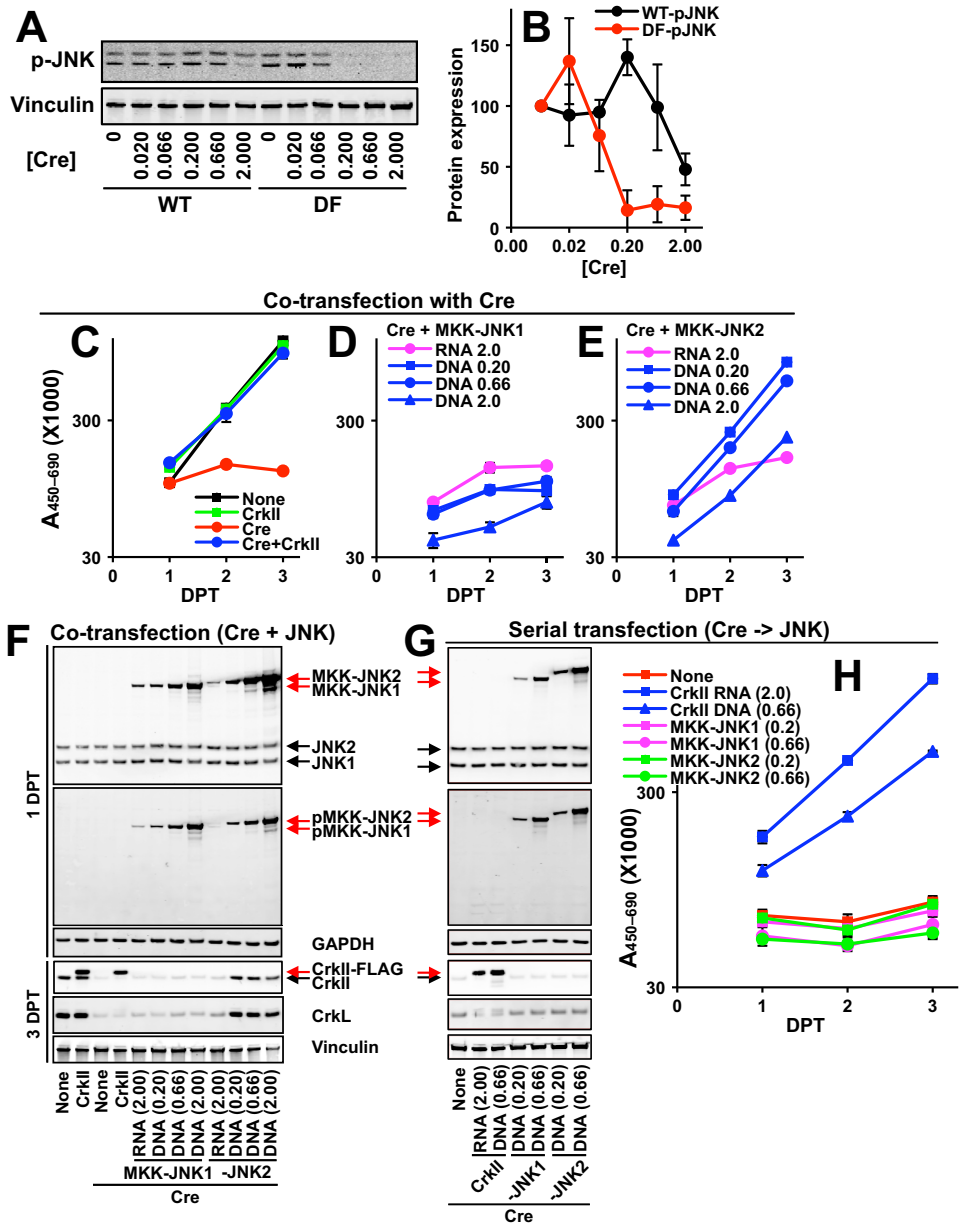

FIGURE 8. **Failed rescue of cell proliferation by JNK activation.** *A* and *B*, T antigen-immortalized wild-type (*WT*) and *Crk/CrkL* double-floxed (*DF*) fibroblasts were transfected with different concentrations of *synCre* (μg in 10 μl cell suspension), and protein levels of phosphorylated JNKs were compared. Protein bands for phosphorylated JNKs were quantified using the Odyssey system, and their mean ± S.D. values at different *synCre* concentrations are shown. *C–H*, proliferation of T antigen-immortalized Crk/CrkL double-floxed (*DF*) fibroblasts co-transfected with *synCre* (0.2 μg) plus CrkII (2 μg *synRNA*) (*D*) or different concentrations (μg) of *synRNA* or DNA for constitutively active JNKs, MKK-JNK1 (*D*) and MKK-JNK2 (*E*) was measured using WST-1. *F*, total cell lysates were obtained from cells co-transfected with *synCre* plus constitutively active JNKs for Western blot analyses. Protein levels of JNKs and phosphorylated JNKs at 1 DPT, and those of Crk and CrkL at 3 DPT are shown. *G*, total cell lysates were obtained from cells serially transfected with *synCre* first and 16 h later with constitutively active JNKs for Western blot analyses. Protein levels of JNKs and phosphorylated JNKs at 1 DPT and those of Crk and CrkL at 3 DPT are shown. *H*, proliferation of cells that were serially transfected first with *synCre* (0.2 μg) and 16 h later with different concentrations (μg) of constitutively active JNKs was measured using WST-1.

mediators of Crk and CrkL functions may need to be developed to understand their complex functions. Our findings help provide a useful starting point for these approaches.

Formation of adherens junctions and subsequent cell cluster formation in addition to reduced cell motility in the absence of Crk and CrkL may provide important insights into biological functions of Crk and CrkL. Failure of migrating neurons to pass through earlier born neurons in the preplate region of the developing brain in *reeler* (53) and brain-specific *Crk/CrkL* knock-out mice (51) might have been caused by aberrant formation of cell-to-cell junctions among earlier born neurons in addition to defective cell motility of migrating neurons. On the other hand, it is likely that the inability of T cells lacking Crk and CrkL to cross an endothelial barrier in CD4-specific *Crk/CrkL* knock-out mice is mainly caused by defective chemotaxis and adhesion of migrating T cells but not by potential changes in formation of cell-to-cell junctions among endothelial cells (50). Recent reports about involvement of Crk and CrkL in epithelial-mesenchymal transition (EMT) (54–57) suggest that reduced cell-to-cell connections among tumor cells and among

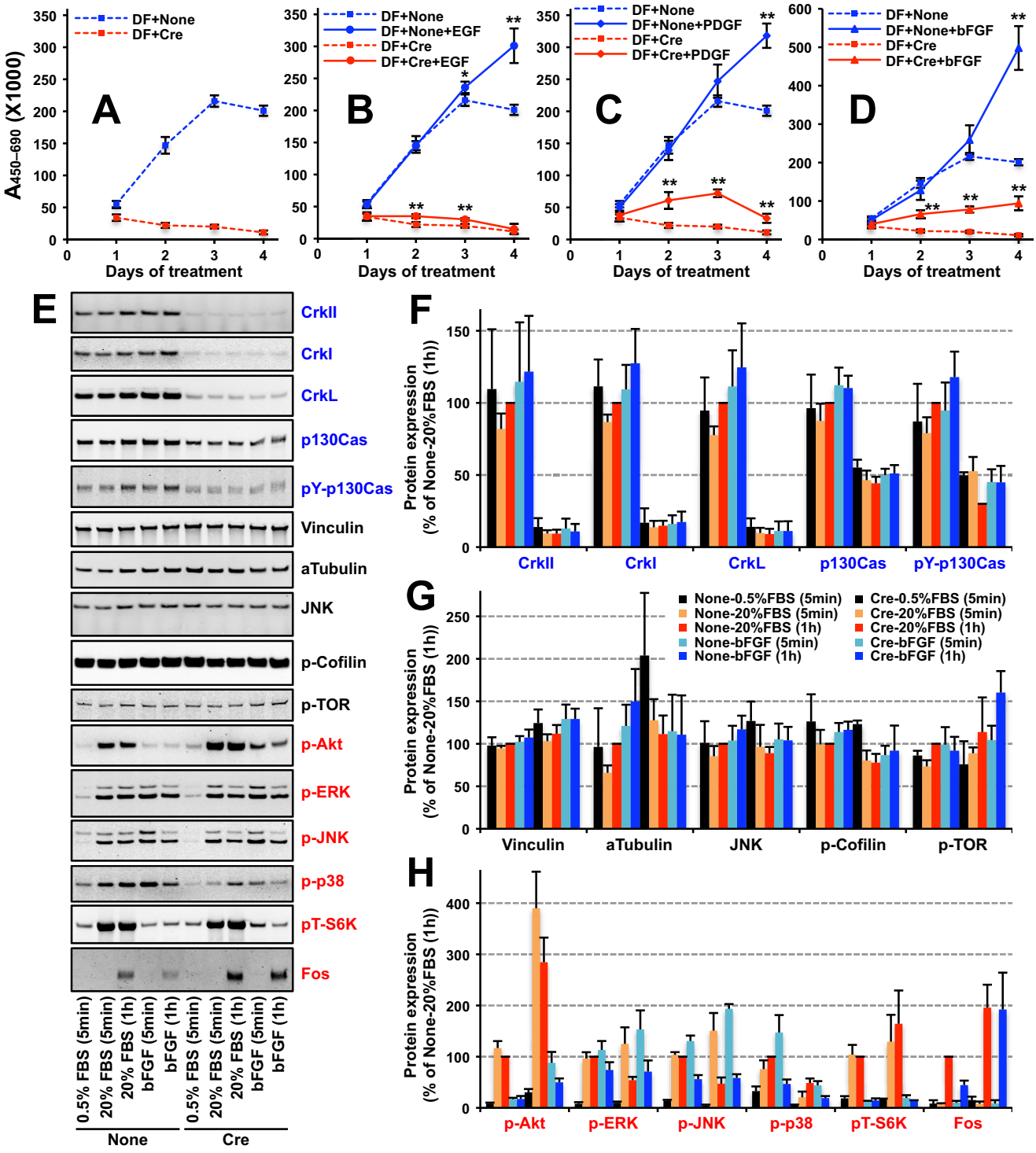

FIGURE 9. **Cell proliferation and activation of signaling molecules in response to serum and growth factors.** *A–D,* T antigen-immortalized *Crk/CrkL* double-floxed (*DF*) fibroblasts were transfected without *synRNA* (*None*) or with *synCre* (0.2 μg in 10 μl cell suspension), plated onto 48-well plates (3000 cells/well), and cultured in normal serum (10% FBS) overnight. The medium was then replaced with DMEM plus low serum (0.5% FBS) with or without growth factors (100 ng/ml EGF, 50 ng/ml basic FGF, or 50 ng/ml PDGF), and cell proliferation for 4 days was measured using WST-1. Data are shown as the mean ± S.D. (*bars*) values. *, $p < 0.05$, **, $p < 0.01$, compared with low serum without growth factor treatment. *E*, T antigen-immortalized Crk/CrkL double-floxed (*DF*) fibroblasts were transfected with *synCre* (0.2 μg in 10 μl cell suspension) and cultured in normal serum (10% FBS) for 2 days. The medium was then replaced with DMEM plus low serum (0.5% FBS), and cells were cultured for additional 24 h. Then cells were stimulated with DMEM plus high serum (20% FBS) or 50 ng/ml basic FGF for 5 min or 1 h at 37 °C, and total cell lysates were obtained for Western blot analyses. *F–H*, protein bands were quantified using the Odyssey system, calculated as percentages of the control (*None* stimulated with 20% FBS for 1 h), and their mean ± S.D. values are shown. Whereas levels of CrkII, CrkI, CrkL, p130Cas, and phosphorylated p130Cas substantially decreased by *synCre* transfection, levels of vinculin, α-tubulin, JNK, phosphorylated cofilin, and phosphorylated TOR did not change by *synCre* transfection.

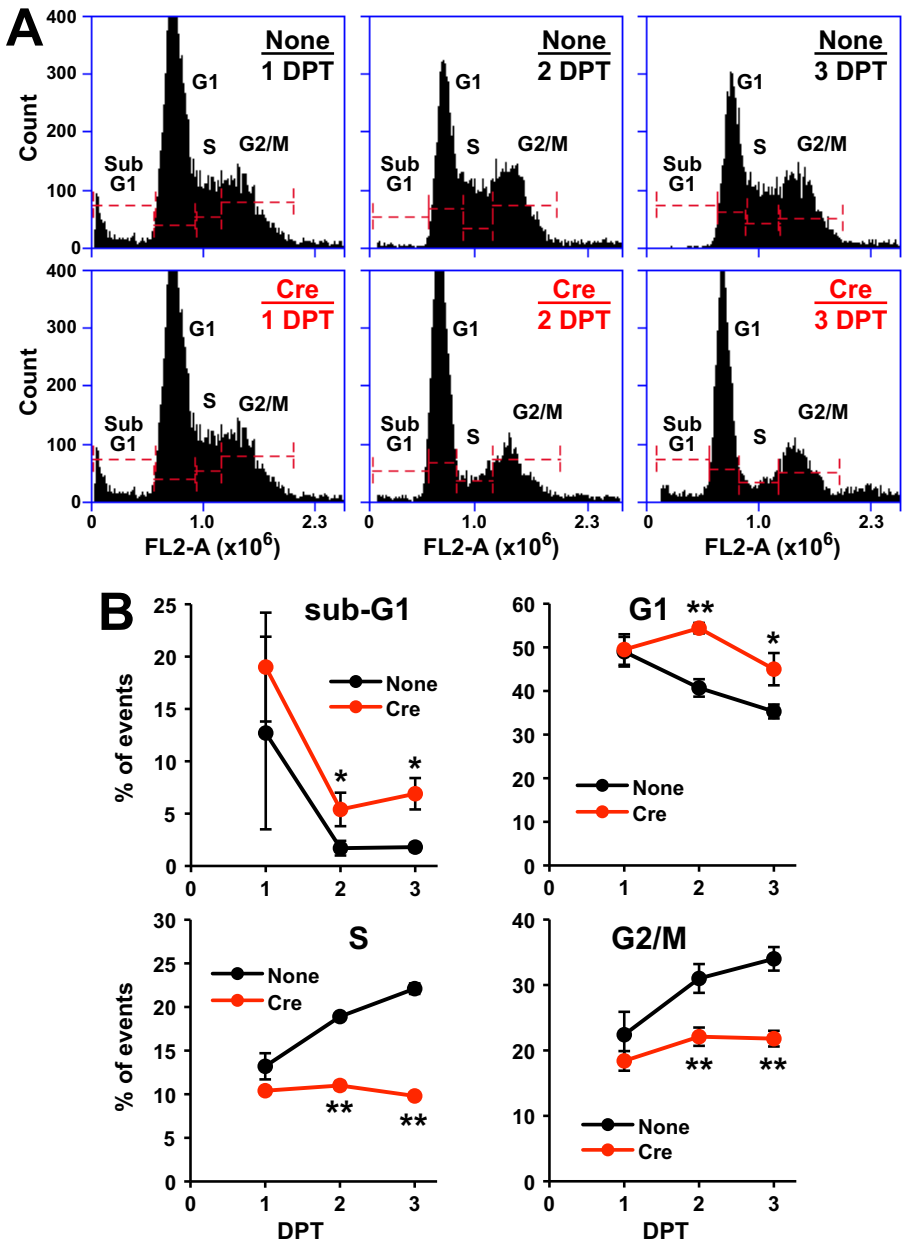

FIGURE 10. **Cell cycle analysis.** T antigen-immortalized *Crk/CrkL* double-floxed (*DF*) fibroblasts were transfected without *synRNA* (*None*) or with *synCre* (0.2 μg in 10 μl cell suspension), cultured, and fixed with ethanol at the indicated DPT for flow cytometry analyses using propidium iodide. Experiments were done in triplicate for each group. *A*, histograms of representative propidium iodide staining are shown. *B*, percentages of events for cell cycle phases are calculated, and their mean ± S.D. values are shown. *, $p < 0.05$; **, $p < 0.01$, compared with control.

endothelial cells in addition to increased motility and invasiveness of tumor cells may contribute to metastasis and poor prognosis of human cancers with elevated levels of Crk and CrkL. Our studies bring significant insights into Crk/CrkL biology, but extensive and combined *in vitro* and *in vivo* studies on Crk and CrkL are still needed to uncover the mechanisms underlying various biological functions of Crk and CrkL in development, tumorigenesis, and metastasis.

Experimental Procedures

Generation of Immortalized Mouse Embryonic Fibroblasts and Electroporation of Cells with Synthetic mRNA—Mouse embryonic fibroblasts were prepared from single or double-floxed Crk/CrkL mouse embryos as previously reported (58). All mouse studies were carried out according to the protocols approved by the Institutional Animal Care and Use Committee at the Children's Hospital of Philadelphia Research Institute. To immortalize fibroblasts, they were either transfected with SV40 large T antigen (22) or passaged according to the 3T3 protocol. Generation of a variety of *Crk* and *CrkL* constructs with the epitope tag FLAG was previously described (21). All the FLAG-tagged constructs in the pLVX-IRES-mCherry vector (Clontech) were subcloned into the pcDNA3.1/myc-His B vector (Invitrogen) for *in vitro* transcription using the T7 promoter. Wild-type, constitutively active, and constitutively inactive *JNK1* and *JNK2* constructs with the FLAG tag deposited by

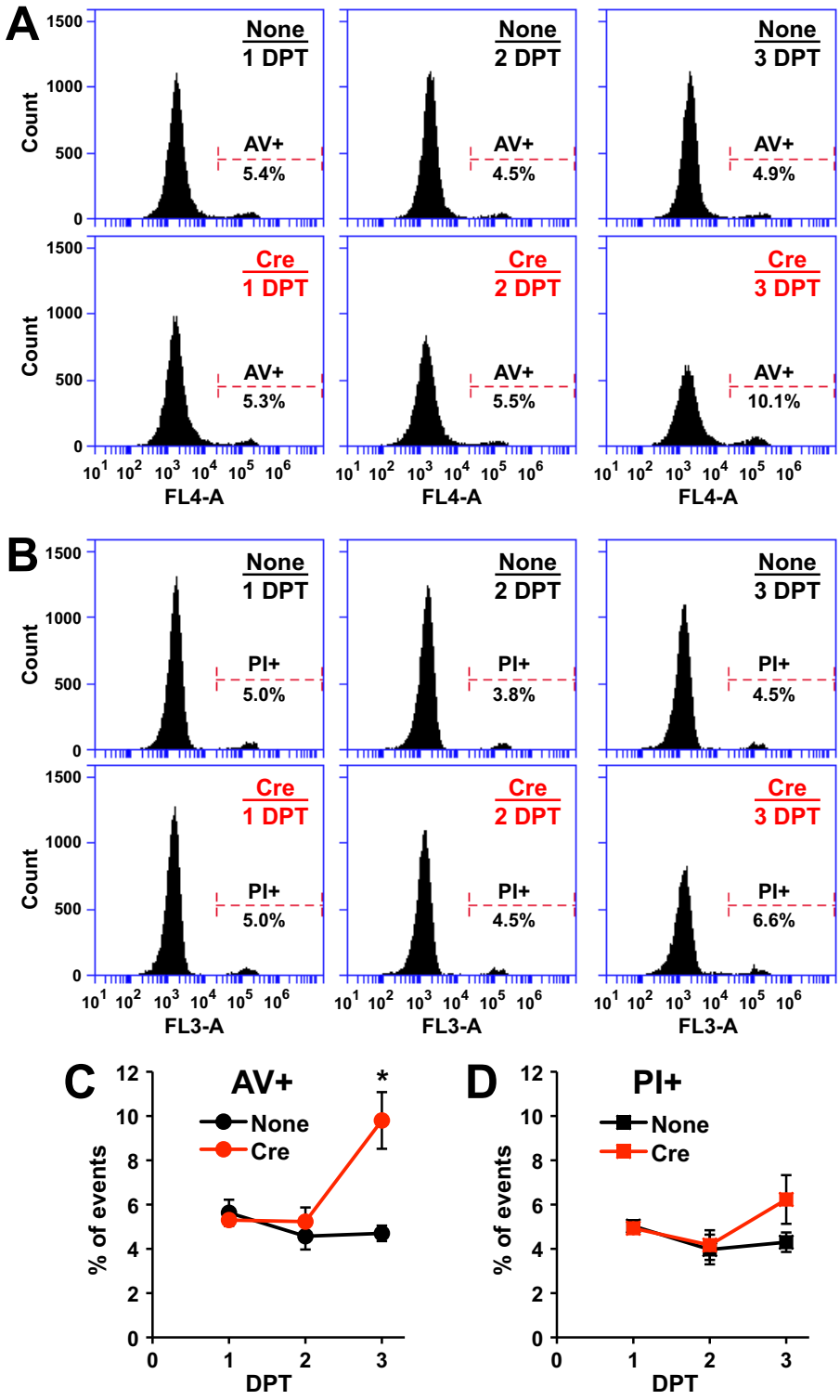

FIGURE 11. **Cell death analysis.** T antigen-immortalized *Crk/CrkL* double-floxed (*DF*) fibroblasts were transfected without *synRNA* (*None*) or with *synCre* (0.2 μg in 10 μl cell suspension), cultured, and harvested at the indicated DPT for flow cytometry analyses using annexin V and propidium iodide to detect apoptosis and necrosis, respectively. Experiments were done in triplicate for each group. *A* and *B*, three separate experiments for annexin V staining were done, and representative histograms for annexin V (*A*) and propidium iodide staining (*B*) are shown. *C* and *D*, percentages of annexin V (*AV*)-positive (*C*) and propidium iodide (*PI*)-positive cells (*D*) are calculated, and their mean ± S.D. values are shown. *, $p < 0.05$, compared with control.

Roger Davis were obtained from Addgene, and their gene names and plasmid numbers are as follows: *Jnk1a1* (13798), *Jnk2a2* (13755), *MKK7B2Jnk1a1* (19726), *MKK7B2Jnk2a2* (19727), *Jnk1a1(apf)* (13846), and *Jnk2a2(apf)* (13761). Synthetic messenger RNAs (*synRNA*) were synthesized *in vitro* using the Megascript T7 reaction (Invitrogen) together with pseudo-UTP and methyl-CTP and the EPAP poly-A tailing system (Ambion) to increase stability and translation (23, 24). For

transfection, fibroblasts were harvested and counted, and 1×10^5 cells were gently mixed with the indicated amounts (μg in 10 μl cell suspension) of synthetic mRNA or DNA, placed in a 10-μl Neon tip, and electroporated with a single pulse at 1350 V for 30 ms using the Neon transfection system (Life Technologies). Transfected cells were seeded onto 48-well plates, 8-well culture slides, 35-mm dishes, and 60-mm dishes for analyses of cell proliferation, immunocytochemistry, protein expression, and flow cytometry, respectively.

Cell Proliferation Assay Using WST-1—Cell proliferation was measured using cleavage of the tetrazolium salt WST-1 (Roche Applied Science) into a water-soluble formazan by cellular enzymes. Cells were seeded in triplicate at 3×10^3 cells/well onto 48-well plates after transfection. To measure cell proliferation, cells were incubated for 2 h in a CO_2 incubator with 200 μl/well of fresh culture medium plus 20 μl/well of WST-1 stock solution provided by the manufacturer. As a background control, WST-1 was added to the medium without cells. At the end of the incubation, the conditioned medium was mixed for 1 min on a shaker, and absorbances were read using the Infinite M200 PRO NanoQuant microplate reader (Tecan) at 450 and 690 nm as measurement and reference wavelengths, respectively. The reference value was subtracted from the measurement value, and the $A_{450-690}$ value was multiplied by 1000 for easy presentation. Results were plotted on a graph using Microsoft Excel with the x axis for DPT and the y axis for $A_{450-690}$ in the logarithmic scale. An exponential trend line was obtained by using the Microsoft Excel program, and the slope of the trend line, which is the coefficient of x, is presented as the rate for exponential cell growth.

Crystal Violet Staining—To visualize cells that have grown in multiwell plates, cells were first washed with PBS and fixed with 4% (w/v) paraformaldehyde plus 4% (w/v) sucrose in PBS. Cells were then stained with 0.1% (w/v) crystal violet for 10 min at room temperature. Cells were washed twice with nanopure water and dried completely. Images of stained cells were captured using the Olympus MVX10 macroscope with a DP71 digital color camera and imported into Adobe Photoshop CS3 for analysis.

Immunocytochemistry and Measurement of Cytoplasmic and Nuclear Areas—Immunostaining of fibroblasts cultured on 8-well culture slides was carried out as previously reported (21). Images of immunostained cells were captured using a Nikon 90i microscope equipped with Roper EZ monochrome and DS-Fi1 color cameras. Quantitative assessments of *synRNA* transfection efficiency and cell morphology were performed by the fluorescence imaging-based method using the Object Count function of the Nikon NIS element program as we described previously (21). To quantify the efficiency of *synRNA* transfection, both GFP and DAPI images of cells were taken throughout the entire area of the well. Images of a minimum of 24 different fields of view were taken for analysis of each sample. Both DAPI-positive objects and DAPI/GFP-positive objects were counted and used to calculate the percentage of GFP-positive cells. To quantify areas of the cytoplasm and nucleus, GFP and DAPI images of cells were taken throughout the entire area of the well. Areas and numbers of DAPI-positive objects were calculated to obtain the average size of the nucleus for each field of view. Then the total area of cells with GFP signals was divided by the number of DAPI-positive objects to obtain the average size of the cytoplasm for each field of view. The values for all the fields of view ($n = 24$ for control cells; $n = 17$ for *synCre*-transfected cells) were combined to calculate the overall sizes of the nucleus and cytoplasm. High magnification images of cells were captured using an Olympus IX70 inverted microscope equipped with Deltavision deconvolution software at the Cell and Developmental Biology Microscopy Core, Perelman School of Medicine at the University of Pennsylvania. Images were processed using FiJi (59) followed by the Nikon NIS element program.

Scratch Wound Healing Assay—Fibroblasts were transfected with *synRNA*, plated on culture slides, and cultured for 2 days. Then a wound was created using a micropipette tip to scratch through the middle of the cell monolayer, and migration of cells into the gap at the wound site was monitored for 24 h. Cells were fixed and stained with a heat shock protein 90 (HSP90) antibody and DAPI to visualize the cytoplasm and nucleus of migrated cells. After fluorescence images were taken using a Nikon 90i microscope, a ROI of 2230×1000 μm was drawn as the original wound gap using the Nikon NIS element program. DAPI-stained objects were counted using the program for the whole image and for the ROI, and the percentage of cells that migrated to the ROI was calculated for each image.

Western Blot Analysis—Preparation of lysates of fibroblasts and Western blot analyses using the Odyssey infrared imaging system (Li-Cor Biosciences) were described previously (21). Protein bands from at least three Western analyses were quantified using the Odyssey system, and their mean $\pm$ S.D. values are shown in the graph. In addition to the previously described antibodies, the following antibodies were used: antibodies for phosphorylated MAP kinases, p-ERK (pTEpY, V8031), p-JNK (pTPpY, V7931), and p-p38 (pTGpY, V1211) were from Promega; anti-JNK1 antibody (554286) was from BD Biosciences; anti-JNK2 antibody (sc-7345) was from Santa Cruz Biotechnology.

Stimulation of Cells with Serum and Growth Factors—Fibroblasts were electroporated with *synRNA* and plated onto 48-well culture plates at low densities (3000 cells/well) in DMEM plus 10% FBS. One day later the medium was replaced with DMEM plus 0.5% FBS supplemented with growth factors (100 ng/ml EGF (Gibco, PHG0314), 50 ng/ml basic FGF (Gibco, 13256-029), 50 ng/ml PDGF (Millipore, GF149), or 100 ng/ml IGF-I (Gibco, PHG0078)). Cell proliferation was measured every day for 4 days using WST-1 (Roche Applied Science). To examine activation of signal transduction pathways, fibroblasts were electroporated with *synRNA*, plated onto 60-mm dishes, and incubated with DMEM plus 10% FBS for 2 days. Then the medium was removed, and cells were incubated with DMEM plus 0.5% FBS for 24 h before treatment with 20% FBS or 50 ng/ml basic FGF in DMEM for 5 min or 1 h. Cell lysates were prepared for Western blot analyses using the Odyssey infrared imaging system (Li-Cor Biosciences).

Flow Cytometry—*Crk/CrkL* double-floxed fibroblasts were electroporated with *synCre* and plated onto 60-mm culture dishes. Subconfluent fibroblasts were harvested at the indicated time points by trypsin-EDTA treatment and centrifugation at

1600 × *g* for 5 min and resuspended in cold Dulbecco's PBS. For cell cycle analysis, cells were fixed by adding cold 70% ethanol dropwise to the cell pellet while gently vortexing and incubating on ice for 15 min. The cell pellet was washed twice with Dulbecco's PBS and treated with DNase-free RNase (Roche Applied Science) at room temperature for 10 min. Then, propidium iodide (Calbiochem) was added to the cell suspension to a final concentration of 10 μg/ml and cells were analyzed by flow cytometry using Accuri C6 (BD Biosciences). For cell death analysis, cells were harvested, resuspended in annexin V binding buffer (BD Biosciences), and stained with allophycocyanin (APC)-annexin V (BD Biosciences) and propidium iodide (a final concentration of 0.05 μg/ml) for flow cytometry with Accuri C6 (BD Biosciences).

Statistical Analysis—All quantitative data were presented as mean ± S.D. Statistical analyses of data were carried out using unpaired two-tailed Student's *t* test for comparison between two experimental groups. Differences were considered to be significant when probability (*p*) values were <0.05.

Author Contributions—T. P. and T. C. designed the study, analyzed the results, and wrote the paper. T. P. conducted all the experiments. M. K. and T. P. conducted flow cytometry experiments and interpreted the results. All authors analyzed the results and approved the final version of the manuscript.

Acknowledgments—We thank Hanna Li for technical assistance. We also thank Jessica M. Y. Ng, Grace Tan, and Mai Dang for critical reading of the manuscript. We also acknowledge the editing services of the Medical Writing Center at Children's Mercy Kansas City.

References

1. Mayer, B. J., Hamaguchi, M., and Hanafusa, H. (1988) Characterization of p47gag-crk, a novel oncogene product with sequence similarity to a putative modulatory domain of protein-tyrosine kinases and phospholipase C. *Cold Spring Harb. Symp. Quant. Biol.* **53,** 907–914
2. Kumar, S., Fajardo, J. E., Birge, R. B., and Sriram, G. (2014) Crk at the quarter century mark: perspectives in signaling and cancer. *J. Cell. Biochem.* **115,** 819–825
3. Matsuda, M., Tanaka, S., Nagata, S., Kojima, A., Kurata, T., and Shibuya, M. (1992) Two species of human CRK cDNA encode proteins with distinct biological activities. *Mol. Cell. Biol.* **12,** 3482–3489
4. Senechal, K., Halpern, J., and Sawyers, C. L. (1996) The CRKL adaptor protein transforms fibroblasts and functions in transformation by the BCR-ABL oncogene. *J. Biol. Chem.* **271,** 23255–23261
5. Yamada, S., Yanamoto, S., Kawasaki, G., Rokutanda, S., Yonezawa, H., Kawakita, A., and Nemoto, T. K. (2011) Overexpression of CRKII increases migration and invasive potential in oral squamous cell carcinoma. *Cancer Lett.* **303,** 84–91
6. Wang, J., Che, Y. L., Li, G., Liu, B., Shen, T. M., Wang, H., and Linghu, H. (2011) Crk and CrkL present with different expression and significance in epithelial ovarian carcinoma. *Mol. Carcinog.* **50,** 506–515
7. Nishihara, H., Tanaka, S., Tsuda, M., Oikawa, S., Maeda, M., Shimizu, M., Shinomiya, H., Tanigami, A., Sawa, H., and Nagashima, K. (2002) Molecular and immunohistochemical analysis of signaling adaptor protein Crk in human cancers. *Cancer Lett.* **180,** 55–61
8. Miller, C. T., Chen, G., Gharib, T. G., Wang, H., Thomas, D. G., Misek, D. E., Giordano, T. J., Yee, J., Orringer, M. B., Hanash, S. M., and Beer, D. G. (2003) Increased C-CRK proto-oncogene expression is associated with an aggressive phenotype in lung adenocarcinomas. *Oncogene* **22,** 7950–7957
9. Wang, Y., Dong, Q. Z., Fu, L., Stoecker, M., Wang, E., and Wang, E. H. (2013) Overexpression of CRKL correlates with poor prognosis and cell proliferation in non-small cell lung cancer. *Mol Carcinog* **52,** 890–899
10. Fathers, K. E., Bell, E. S., Rajadurai, C. V., Cory, S., Zhao, H., Mourskaia, A., Zuo, D., Madore, J., Monast, A., Mes-Masson, A. M., Grosset, A. A., Gaboury, L., Hallet, M., Siegel, P., and Park, M. (2012) Crk adaptor proteins act as key signaling integrators for breast tumorigenesis. *Breast Cancer Res.* **14,** R74
11. Rodrigues, S. P., Fathers, K. E., Chan, G., Zuo, D., Halwani, F., Meterissian, S., and Park, M. (2005) CrkI and CrkII function as key signaling integrators for migration and invasion of cancer cells. *Mol. Cancer Res.* **3,** 183–194
12. Wang, J., Chen, X., Li, P., Su, L., Yu, B., Cai, Q., Li, J., Yu, Y., Liu, B., and Zhu, Z. (2013) CRKL promotes cell proliferation in gastric cancer and is negatively regulated by miR-126. *Chem. Biol. Interact.* **206,** 230–238
13. Takino, T., Nakada, M., Miyamori, H., Yamashita, J., Yamada, K. M., and Sato, H. (2003) CrkI adapter protein modulates cell migration and invasion in glioblastoma. *Cancer Res.* **63,** 2335–2337
14. Wang, L., Tabu, K., Kimura, T., Tsuda, M., Linghu, H., Tanino, M., Kaneko, S., Nishihara, H., and Tanaka, S. (2007) Signaling adaptor protein Crk is indispensable for malignant feature of glioblastoma cell line KMG4. *Biochem. Biophys. Res. Commun.* **362,** 976–981
15. Linghu, H., Tsuda, M., Makino, Y., Sakai, M., Watanabe, T., Ichihara, S., Sawa, H., Nagashima, K., Mochizuki, N., and Tanaka, S. (2006) Involvement of adaptor protein Crk in malignant feature of human ovarian cancer cell line MCAS. *Oncogene* **25,** 3547–3556
16. Watanabe, T., Tsuda, M., Makino, Y., Ichihara, S., Sawa, H., Minami, A., Mochizuki, N., Nagashima, K., and Tanaka, S. (2006) Adaptor molecule Crk is required for sustained phosphorylation of Grb2-associated binder 1 and hepatocyte growth factor-induced cell motility of human synovial sarcoma cell lines. *Mol Cancer Res.* **4,** 499–510
17. Yanagi, H., Wang, L., Nishihara, H., Kimura, T., Tanino, M., Yanagi, T., Fukuda, S., and Tanaka, S. (2012) CRKL plays a pivotal role in tumorigenesis of head and neck squamous cell carcinoma through the regulation of cell adhesion. *Biochem. Biophys. Res. Commun.* **418,** 104–109
18. Yeung, C. L., Ngo, V. N., Grohar, P. J., Arnaldez, F. I., Asante, A., Wan, X., Khan, J., Hewitt, S. M., Khanna, C., Staudt, L. M., and Helman, L. J. (2013) Loss-of-function screen in rhabdomyosarcoma identifies CRKL-YES as a critical signal for tumor growth. *Oncogene* **32,** 5429–5438
19. Sriram, G., and Birge, R. B. (2010) Emerging roles for crk in human cancer. *Genes Cancer* **1,** 1132–1139
20. Tsuda, M., and Tanaka, S. (2012) Roles for crk in cancer metastasis and invasion. *Genes Cancer* **3,** 334–340
21. Park, T. J., and Curran, T. (2014) Essential roles of Crk and CrkL in fibroblast structure and motility. *Oncogene* **33,** 5121–5132
22. Koptyra, M., Park, T. J., and Curran, T. (2016) Crk and CrkL are required for cell transformation by v-fos and v-ras. *Mol Carcinog* **55,** 97–104
23. Warren, L., Manos, P. D., Ahfeldt, T., Loh, Y. H., Li, H., Lau, F., Ebina, W., Mandal, P. K., Smith, Z. D., Meissner, A., Daley, G. Q., Brack, A. S., Collins, J. J., Cowan, C., Schlaeger, T. M., and Rossi, D. J. (2010) Highly efficient reprogramming to pluripotency and directed differentiation of human cells with synthetic modified mRNA. *Cell Stem Cell* **7,** 618–630
24. Kuhn, A. N., Beiβert, T., Simon, P., Vallazza, B., Buck, J., Davies, B. P., Tureci, O., and Sahin, U. (2012) mRNA as a versatile tool for exogenous protein expression. *Curr. Gene Ther.* **12,** 347–361
25. Batt, D. B., and Roberts, T. M. (1998) Cell density modulates protein-tyrosine phosphorylation. *J. Biol. Chem.* **273,** 3408–3414
26. Lamorte, L., Royal, I., Naujokas, M., and Park, M. (2002) Crk adapter proteins promote an epithelial-mesenchymal-like transition and are required for HGF-mediated cell spreading and breakdown of epithelial adherens junctions. *Mol. Biol. Cell* **13,** 1449–1461
27. Mortazavi, F., Dubinett, S., and Rettig, M. (2011) c-Crk proto-oncogene contributes to transcriptional repression of p120-catenin in non-small cell lung cancer cells. *Clin. Exp. Metastasis* **28,** 391–404
28. Loonstra, A., Vooijs, M., Beverloo, H. B., Allak, B. A., van Drunen, E., Kanaar, R., Berns, A., and Jonkers, J. (2001) Growth inhibition and DNA damage induced by Cre recombinase in mammalian cells. *Proc. Natl. Acad. Sci. U.S.A.* **98,** 9209–9214

29. Pfeifer, A., Brandon, E. P., Kootstra, N., Gage, F. H., and Verma, I. M. (2001) Delivery of the Cre recombinase by a self-deleting lentiviral vector: efficient gene targeting *in vivo*. *Proc. Natl. Acad. Sci. U.S.A.* **98,** 11450–11455
30. Bell, E. S., and Park, M. (2012) Models of crk adaptor proteins in cancer. *Genes Cancer* **3,** 341–352
31. Isakov, N. (2008) A new twist to adaptor proteins contributes to regulation of lymphocyte cell signaling. *Trends Immunol* **29,** 388–396
32. Birge, R. B., Kalodimos, C., Inagaki, F., and Tanaka, S. (2009) Crk and CrkL adaptor proteins: networks for physiological and pathological signaling. *Cell Commun. Signal* **7,** 13
33. Kodama, H., Fukuda, K., Takahashi, E., Tahara, S., Tomita, Y., Ieda, M., Kimura, K., Owada, K. M., Vuori, K., and Ogawa, S. (2003) Selective involvement of p130Cas/Crk/Pyk2/c-Src in endothelin-1-induced JNK activation. *Hypertension* **41,** 1372–1379
34. Salameh, A., Galvagni, F., Bardelli, M., Bussolino, F., and Oliviero, S. (2005) Direct recruitment of CRK and GRB2 to VEGFR-3 induces proliferation, migration, and survival of endothelial cells through the activation of ERK, AKT, and JNK pathways. *Blood* **106,** 3423–3431
35. Ishimaru, S., Ueda, R., Hinohara, Y., Ohtani, M., and Hanafusa, H. (2004) PVR plays a critical role via JNK activation in thorax closure during *Drosophila* metamorphosis. *EMBO J.* **23,** 3984–3994
36. Mochizuki, N., Ohba, Y., Kobayashi, S., Otsuka, N., Graybiel, A. M., Tanaka, S., and Matsuda, M. (2000) Crk activation of JNK via C3G and R-Ras. *J. Biol. Chem.* **275,** 12667–12671
37. Tanaka, S., Ouchi, T., and Hanafusa, H. (1997) Downstream of Crk adaptor signaling pathway: activation of Jun kinase by v-Crk through the guanine nucleotide exchange protein C3G. *Proc. Natl. Acad. Sci. U.S.A.* **94,** 2356–2361
38. Lamorte, L., Kamikura, D. M., and Park, M. (2000) A switch from p130Cas/Crk to Gab1/Crk signaling correlates with anchorage independent growth and JNK activation in cells transformed by the Met receptor oncoprotein. *Oncogene* **19,** 5973–5981
39. Rodrigues, G. A., Park, M., and Schlessinger, J. (1997) Activation of the JNK pathway is essential for transformation by the Met oncogene. *EMBO J.* **16,** 2634–2645
40. Lei, K., Nimnual, A., Zong, W. X., Kennedy, N. J., Flavell, R. A., Thompson, C. B., Bar-Sagi, D., and Davis, R. J. (2002) The Bax subfamily of Bcl2-related proteins is essential for apoptotic signal transduction by c-Jun NH_2-terminal kinase. *Mol. Cell. Biol.* **22,** 4929–4942
41. Paski, S. C., and Xu, Z. (2002) Growth factor stimulated cell proliferation is accompanied by an elevated labile intracellular pool of zinc in 3T3 cells. *Can. J. Physiol. Pharmacol.* **80,** 790–795
42. Deng, Y., Zhang, M., and Riedel, H. (2008) Mitogenic roles of Gab1 and Grb10 as direct cellular partners in the regulation of MAP kinase signaling. *J. Cell. Biochem.* **105,** 1172–1182
43. Li, F., Liu, S., Ouyang, Y., Fan, C., Wang, T., Zhang, C., Zeng, B., Chai, Y., and Wang, X. (2012) Effect of celecoxib on proliferation, collagen expression, ERK1/2 and SMAD2/3 phosphorylation in NIH/3T3 fibroblasts. *Eur. J. Pharmacol.* **678,** 1–5
44. Antoku, S., and Mayer, B. J. (2009) Distinct roles for Crk adaptor isoforms in actin reorganization induced by extracellular signals. *J. Cell Sci.* **122,** 4228–4238
45. Huang, S., and Ingber, D. E. (2002) A discrete cell cycle checkpoint in late G_1 that is cytoskeleton-dependent and MAP kinase (Erk)-independent. *Exp. Cell Res.* **275,** 255–264
46. Huang, S., Chen, C. S., and Ingber, D. E. (1998) Control of cyclin D1, p27(Kip1), and cell cycle progression in human capillary endothelial cells by cell shape and cytoskeletal tension. *Mol. Biol. Cell* **9,** 3179–3193
47. Lohez, O. D., Reynaud, C., Borel, F., Andreassen, P. R., and Margolis, R. L. (2003) Arrest of mammalian fibroblasts in G_1 in response to actin inhibition is dependent on retinoblastoma pocket proteins but not on p53. *J. Cell Biol.* **161,** 67–77
48. George, B., Fan, Q., Dlugos, C. P., Soofi, A. A., Zhang, J., Verma, R., Park, T. J., Wong, H., Curran, T., Nihalani, D., and Holzman, L. B. (2014) Crk1/2 and CrkL form a hetero-oligomer and functionally complement each other during podocyte morphogenesis. *Kidney Int.* **85,** 1382–1394
49. Hallock, P. T., Xu, C. F., Park, T. J., Neubert, T. A., Curran, T., and Burden, S. J. (2010) Dok-7 regulates neuromuscular synapse formation by recruiting Crk and Crk-L. *Genes Dev.* **24,** 2451–2461
50. Huang, Y., Clarke, F., Karimi, M., Roy, N. H., Williamson, E. K., Okumura, M., Mochizuki, K., Chen, E. J., Park, T. J., Debes, G. F., Zhang, Y., Curran, T., Kambayashi, T., and Burkhardt, J. K. (2015) CRK proteins selectively regulate T cell migration into inflamed tissues. *J. Clin. Invest.* **125,** 1019–1032
51. Park, T. J., and Curran, T. (2008) Crk and Crk-like play essential overlapping roles downstream of disabled-1 in the Reelin pathway. *J. Neurosci.* **28,** 13551–13562
52. Cheng, S., Guo, J., Yang, Q., and Han, L. (2015) Crk-like adapter protein is required for TGF-β-induced AKT and ERK-signaling pathway in epithelial ovarian carcinomas. *Tumour Biol.* **36,** 915–919
53. Magdaleno, S., Keshvara, L., and Curran, T. (2002) Rescue of ataxia and preplate splitting by ectopic expression of Reelin in reeler mice. *Neuron* **33,** 573–586
54. Cheng, S., Guo, J., Yang, Q., and Yang, X. (2015) Crk-like adapter protein regulates CCL19/CCR7-mediated epithelial-to-mesenchymal transition via ERK signaling pathway in epithelial ovarian carcinomas. *Med. Oncol.* **32,** 47
55. Han, G., Wu, D., Yang, Y., Li, Z., Zhang, J., and Li, C. (2015) CrkL meditates CCL20/CCR6-induced EMT in gastric cancer. *Cytokine* **76,** 163–169
56. Matsumoto, R., Tsuda, M., Wang, L., Maishi, N., Abe, T., Kimura, T., Tanino, M., Nishihara, H., Hida, K., Ohba, Y., Shinohara, N., Nonomura, K., and Tanaka, S. (2015) Adaptor protein CRK induces epithelial-mesenchymal transition and metastasis of bladder cancer cells through HGF/c-Met feedback loop. *Cancer Sci.* **106,** 709–717
57. Elmansuri, A. Z., Tanino, M. A., Mahabir, R., Wang, L., Kimura, T., Nishihara, H., Kinoshita, I., Dosaka-Akita, H., Tsuda, M., and Tanaka, S. (2016) Novel signaling collaboration between TGF-β and adaptor protein Crk facilitates EMT in human lung cancer. *Oncotarget* **7,** 27094–27107
58. Park, T. J., Boyd, K., and Curran, T. (2006) Cardiovascular and craniofacial defects in Crk-null mice. *Mol. Cell. Biol.* **26,** 6272–6282
59. Schindelin, J., Arganda-Carreras, I., Frise, E., Kaynig, V., Longair, M., Pietzsch, T., Preibisch, S., Rueden, C., Saalfeld, S., Schmid, B., Tinevez, J. Y., White, D. J., Hartenstein, V., Eliceiri, K., Tomancak, P., and Cardona, A. (2012) Fiji: an open-source platform for biological-image analysis. *Nat. Methods* **9,** 676–682